IMPACT OF BACKREFLECTIONS ON SINGLE-FIBER BIDIRECTIONAL WAVELENGTH-DIVISION-MULTIPLEXING PASSIVE OPTICAL NETWORKS (WDM-PONs)

By

Shiyu Gao

A thesis submitted to the
Faculty of Graduate and Postdoctoral Studies
in partial fulfillment of the requirements for the degree of
Master of Applied Science

Ottawa-Carleton Institute of Electrical and Computer Engineering
School of Electrical Engineering and Computer Science
Faculty of Engineering
University of Ottawa

January 2013

ABSTRACT

With increased demand for bandwidth-hungry applications such as video-on-demand, wavelength-division-multiplexing passive optical network (WDM-PON) has become a strong contender in overcoming the last mile bottle neck. However, the wide-scale deployment of WDM-PONs has been delayed mainly due to the high cost of wavelength-specific optical components. To realize cost-effective WDM-PONs, various wavelength-independent, so called colorless architectures, have been developed so that all the subscribers can have identical optical network units (ONUs). In such WDM-PONs, however, single-fiber bidirectional transmission results in degradation of system performance caused by interference between the signals and backreflections.

This thesis investigates the impact of backreflections on single-fiber bidirectional WDM-PONs. A WDM-PON with various optical line terminals (OLTs) and colorless ONU configurations is presented. The dependence of the power penalty, caused by backreflections, on a variety of parameters is investigated. This includes parameters such as the source linewidths, receiver bandwidth, transmission line loss (TLL), ONU gain, chirp effect at the ONU and optical return loss (ORL), in various WDM-PON configurations. The WDM-PON with continuous wave (CW) seed light and remodulation schemes are both presented and studied experimentally. The impacts of the backreflections on the single-fiber bidirectional WDM-PON with various OLT and ONU configurations are compared and analyzed accordingly.

TABLE OF CONTENTS

ABSTRACT i

TABLE OF CONTENTS ii

LIST OF ACRONYMS v

LIST OF FIGURES vii

LIST OF TABLES ix

ACKNOWLEDGMENTS x

CHAPTER 1 INTRODUCTION 1

1.1 Research motivation 1

1.2 Thesis objectives & major contributions 3

1.3 Thesis outline 4

CHAPTER 2 WAVELENGTH-DIVISION-MULTIPLEXING PASSIVE OPTICAL NETWORKS (WDM-PONs) 6

2.1 Background overview 6

2.2 PON architectures and standards 9

2.2.1 TDM-PONs 9

2.2.2 WDM-PONs 10

2.2.3 PON standards 13

2.3 WDM-PON technologies 14

2.3.1 State of the art 14

2.3.2 Colorless architectures in WDM-PONs 15

2.3.2.1 Injection-locking of FP-LDs 15

2.3.2.2 Wavelength-seeding of RSOAs *18*

2.3.3 Wavelength-reused remodulation schemes in WDM-PONs 20

2.3.4 Comparison of various colorless architectures in WDM-PONs 23

2.4 Impairments in single-fiber bidirectional WDM-PONs 25

2.4.1 Fiber loss 27

2.4.2 Fiber dispersion 28

2.4.3 Intensity noise from BLS and colorless ONUs 30

2.4.4 Rayleigh backscattering (RB) 31

2.5 Summary 34

CHAPTER 3 INVESTIGATION OF BACKREFLECTIONS IN SINGLE-FIBER BIDIRECTIONAL WDM-PONs 36

3.1 Motivation 36

3.2 Principles of backreflections in WDM-PONs 39

3.2.1 Backreflections I & II 39

3.2.2 Power penalty and optimum ONU gain 42

3.3 Experimental results 46

3.3.1 Experimental setup 47

3.3.2 Characteristics of system components 50

3.3.3 Experimental results in WDM-PON with CW seed light 54

3.3.3.1 Impact of backreflections on RSOA-based WDM-PON *55*

3.3.3.2 Impact of backreflections on FP-LD-based WDM-PON *60*

3.3.3.3 Comparison of impact of backreflections on RSOA- and FP-LD-based WDM-PON *62*

3.3.4 Experimental results in WDM-PON with remodulation scheme 63

3.3.4.1 Evaluation of WDM-PON's performance with remodulation scheme..... 63

3.3.4.2 Impact of backreflections on RSOA-based WDM-PON with remodulation scheme 69

3.3.4.3 Impact of backreflections on FP-LD-based WDM-PON with remodulation scheme 70

3.3.4.4 Comparison of impact of backreflections on WDM-PON with CW seed light and remodulation scheme 71

3.4 Summary and discussion 74

CHAPTER 4 CONCLUSIONS 77

4.1 Thesis summary 77

4.2 Future work 79

BIBLIOGRPHY 81

LIST OF ACRONYMS

A

APON Asynchronous Transfer Mode Passive Optical Network
ASE Amplified Spontaneous Emission
AWG Arrayed Waveguide Grating

B

BER Bit Error Rate
BERT Bit Error Rate Test Set
BLS Broadband Light Source
BPON Broadband Passive Optical Network

C

CATV Community Antenna Television
CLS Centralized Light Source
CO Central Office
CW Continuous Wave

D

DCA Digital Communication Analyzer
DFB-LD Distributed Feedback Laser Diode
DSL Digital Subscriber Line
DWDM Dense Wavelength Division Multiplexing

E

EAM Electro-absorption Modulator
EIN Excess Intensity Noise
EDFA Erbium Doped Fiber Amplifier
EOM Electro-optic Modulator
EPON Ethernet Passive Optical Network
ER Extinction Ratio

F

FBG Fiber Bragg Grating
FP-LD Fabry Pérot Laser Diode
FTTH Fiber-to-the-home
FTTx Fiber-to-the-x
FWM Four-wave Mixing

G

GPON Gigabit Passive Optical Network

I

IRZ Inverse Return-to-zero
ITU International Telecommunication Union

L

LD Laser Diode
LED Light Emission Diode

M

MW-LS Multi-wavelength Light Source

N

NG-PON Next-generation Passive Optical Network
NRZ Non-return-to-zero

O

ODL Optical Delay Line
OOK On–off Keying
OLT Optical Line Terminal
ONU Optical Network Unit
ORL Optical Return Loss

P

PON Passive Optical Network
PRBS Pseudorandom Bit Sequence
PSD Power Spectral Density
PSTN Public-switched Telephone Network
P2MP Point-to-multipoint
P2P Point-to-point

R

RB Rayleigh backscattering
REAM Reflective Electro-absorption Modulator
RIN Relative Intensity Noise
RSOA Reflective Semiconductor Optical Amplifier
RN Remote Node
RZ Return-to-zero

S

SFP Small Form-factor Pluggable
SMF Single-mode Fiber
SMSR Side-mode-suppression- ratio
SNR Signal-to-noise Ratio
SLED Superluminescent Light Emitting Diode
SOA Semiconductor Optical Amplifier

T

TDM Time Division Multiplexing
TLL Transmission Line Loss

V

VOA Variable Optical Attenuator

W

WDM Wavelength Division Multiplexing

X

XG-PON Next-generation Gigabit Passive Optical Network

LIST OF FIGURES

Fig. 2.1 Forecast of the global consumer internet traffic (2011-2016) 7

Fig. 2.2 Various architectures of FTTH 8

Fig. 2.3 Architeture of TDM-PON 9

Fig. 2.4 Architecture of a WDM-PON 11

Fig. 2.5 Evolution of PON standards 13

Fig. 2.6 A WDM-PON with injection-locked FP-LDs by spectrum-sliced ASE light 16

Fig. 2.7 A WDM-PON with wavelength-seeded RSOAs by coherent light 19

Fig. 2.8 Remodulation-based WDM-PON structure employing RSOAs 21

Fig. 2.9 Gain characteristic of the RSOA 22

Fig. 2.10 Options for single-fiber bidirectional transmission: (a) one fiber with two wavelengths; (b) one fiber with one wavelength 26

Fig. 3.1 Backreflections I and II in single-fiber bidirectional WDM-PON access network 39

Fig. 3.2 Reducing the impact of backreflection I by signal amplification at ONU 40

Fig.3.3 Influence of ONU gain on SNR 42

Fig. 3.4 Schematic of the experimental setup 48

Fig. 3.5 Spectrums of the seed light selection from the MW-LS 51

Fig. 3.6 Gain characteristics of RSOA 53

Fig. 3.7 Spectrum of total RIN at mark level for three cases: DFB –LD, ASE and MW-LS injection 55

Fig. 3.8 Power penalty as a function of the ONU gain for different injection sources at OLT (a) all (b) ASE 56

Fig. 3.9 Power penalty versus ONU gain at various ORLs 58
Fig. 3.10 Power penalty as a function of the ONU gain for different receiver bandwidths 59
Fig. 3.11 FP-LD spectrums after injection (a) -3 dBm injected power (b) 0 dBm injected power 61
Fig. 3.12 Power penalty versus ONU gain for -3 dBm and 0 dBm injection powers to the FP-LD 62
Fig. 3.13 Power penalty as a function of ONU gain for identical OLT and different ONUs 63
Fig. 3. 14 Simplified WDM-PON with remodulation scheme 64
Fig. 3.15 EOM response test curve 65
Fig. 3.16 RSOA gain versus input optical power 66
Fig. 3.17 Eye diagrams of upstream signal with various downstream ER 67
Fig. 3.18 Eye diagrams of upstream signal with different downstream signal bit rate 68
Fig. 3.19 Power penalty as a function of ONU gain for different TLLs 69
Fig. 3.20 Power penalty versus ONU gain for -3 dBm and 0 dBm injection powers to the FP-LD 70
Fig. 3.21 Measured eye diagrams at different ONU gains (a) G=5 dB (b) G=9 dB (c) G=14 dB 71
Fig. 3.22 Power penalty as a function of ONU gain for identical OLT and different ONUs 72
Fig. 3.23 Power penalty comparison between CW and modulated signal injection 74

LIST OF TABLES

Table 2.1 Comparison of colorless architectures 24

Table 3.1 Linewidth measurement results..... 72

ACKNOWLEDGMENTS

First and foremost, I would like to express my sincerest gratitude to my supervisor, Professor Hanan Anis, for her constant support, guidance and valuable advices throughout the research work. Her patience, motivation, enthusiasm and immense knowledge have made her as a great mentor. This work would not have been completed without her support and encouragement. I am really fortunate to have Professor Anis as my supervisor.

I am also very thankful to Dr. Hanwu Hu, who was a researcher in our group. I have learned a lot of knowledge from him and obtained valuable experience in the research field. His theoretical insights were crucial for the modeling part of this research work.

Furthermore, my grateful thanks also go to the present and former members in the Photonics Laboratory of University of Ottawa, who are my colleagues as well as my friends. Their strong support and generous help have greatly improved my research work. I feel so lucky to be part of the group.

My deepest appreciation goes to my parents for their unconditional love and understanding. Last but not least, my special thanks go to my beloved husband, Yu Yan, for his boundless love and unquestioning support, all through my life.

CHAPTER 1 INTRODUCTION

1.1 Research motivation

With the rising popularity of the internet and its applications, our life is dominated nowadays by bandwidth-hungry services such as high-definition videos and live streaming. The explosive growth in the demand for higher bandwidth has triggered the introduction of fiber-to-the-home (FTTH) based broadband access networks. Among various FTTH implementations, passive optical network (PON), which can provide very high bandwidths to the customers, appears to be an attractive solution to the access network. Other than offering high bandwidth, a PON system offers a large coverage area, reduced fiber deployment as the result of its point-to-multipoint (P2MP) architecture, and reduced cost of maintenance due to the use of passive components in the network. Incorporating wavelength division multiplexing (WDM) in a PON allows one to support higher bandwidth compared to the standard PON since each wavelength is dedicated to a single subscriber. The WDM-PON offers other advantages such as ease of management and upgradability, strong network security, high flexibility with data and protocol transparency, so that it has been considered by many as a future-proof access technology and an ultimate next-generation FTTH network [1-6]. However, due to the virtual point-to-point (P2P) connection architecture, the WDM-PON system requires expensive wavelength-specified transmitters at the optical line terminal (OLT) which is located at the telecom central office (CO), as well as at the optical network units (ONUs) which are

located at the subscriber premises. Consequently, to realize a cost-competitive WDM-PON, economical solutions must be developed.

A majority of the work in WDM-PONs have focused on the system cost efficiency especially at the user side where cost is most sensitive. To this end, in a successful deployment of the WDM-PON, the ONUs placed in the subscriber premises should be wavelength-independent or wavelength-free, so called the colorless ONUs. Recently, many WDM-PON loopback access networks with colorless ONUs have been proposed [7-18]. In most of these schemes, low-cost lasers or modulators, such as Fabry Pérot laser diodes (FP-LDs), reflective semiconductor optical amplifiers (RSOAs) are located at the ONUs, while a continuous wave (CW) seed light is sent from the OLT to the ONU and then looped back to the receiver at the OLT. This round-trip transmission is achieved by using either two fibers [7–10] or a single fiber [11–18]. Single-fiber loopback transmission is more attractive than two fibers systems as the number of optical fibers used can be reduced resulting in a system cost reduction. Furthermore, there has also been significant interest in reusing the downstream optical signal for the upstream transmission, which is known as the remodulation scheme [9], [19-23]. These configurations eliminate the need for an extra CW seed light, and hence it is more cost-effective. However, such single-fiber bidirectional loopback transmission results in degradation of the signal-to-noise ratio (SNR) of the received signal from the optical beat noises caused by backreflections. It is well known that Rayleigh backscattering (RB) cannot be avoided in optical fiber transmission due to the intrinsic nature of the fiber with microscopic fluctuations of refractive index [24]. In a single-fiber bidirectional WDM-PON, the backreflected up/downstream will beat with its counter-propagating

down/upstream since they share the same wavelength. Moreover, all practical networks will have Fresnel reflections from components and connectors. As a result, it is essential to investigate the impact of backreflections in single-fiber bidirectional WDM-PON access networks, which would help evaluate the system performance and develop the network configurations.

1.2 Thesis objectives & major contributions

The main objective of this thesis is to analyze the system impairments due to optical beat noise between backreflections and the upstream signal in single-fiber bidirectional WDM-PON access networks.

The major contributions of this research are as follows. A single-fiber bidirectional WDM-PON system with backreflection setup to study the backreflection impact is demonstrated, including various seed lights at the OLT such as a distributed feedback laser diode (DFB-LD), a spectrum-sliced amplified spontaneous emission (ASE) source or a filtered multi-wavelength light source (MW-LS), and two kinds of colorless ONUs, which is based on a RSOA or a FP-LD. The dependence of the power penalty caused by the optical beat noise on a variety of parameters such as the source linewidths, receiver bandwidth, transmission line loss (TLL), ONU gain, chirp effect at the ONU and optical return loss (ORL) is intensively investigated in various WDM-PON configurations. The WDM-PON with CW seed light and the remodulation scheme are both presented and studied experimentally. The impacts of the backreflections on the single-fiber

bidirectional WDM-PON with various OLT and ONU configurations are compared and analyzed accordingly.

The original contribution of this research work has been evidenced by the following publications in scientific and engineering journals and conferences:

1. **S. Gao**, H. Hu, A. Atieh, and H. Anis, "Impact of linewidth on system impairment caused by backreflection in WDM PONs," in *Proc. OFC/NFOEC*, paper JThA99, 2008.

2. **S. Gao**, H. Hu, and H. Anis, "Impact of backreflections on single-fiber bidirectional transmission in WDM-PONs*," J. Opt. Commun. Netw*., vol. 3, no. 10, pp. 797–805, Oct. 2011.

1.3 Thesis outline

This thesis investigates the impact of backreflections on single-fiber bidirectional WDM-PONs. The thesis is organized as follows:

Chapter 2 provides an overview of WDM-PONs. It starts with a background of optical access networks and PONs. Then various PON architectures and standards, as well as the evolution towards WDM-PONs, are introduced. In section 2.3, I discuss the main WDM-PON technologies. This section focuses on the solutions to realize cost-effective WDM-PONs, which include colorless architectures such as injection-locking of FP-LDs and wavelength-seeding of RSOAs, as well as wavelength-reused remodulation schemes. Finally in section 2.4, I discuss the main impairments in single-fiber bidirectional WDM-PONs.

Chapter 3 focuses on my experimental research on the system impairment due to the backreflections in single-fiber bidirectional WDM-PON access networks. I begin with a literature review of recent work on the impact of backreflections and point out the insufficiency and drawbacks of these studies which was the motivation of my research. Secondly, I present the basic principles and definitions of backreflections I and II, which are the two dominant backreflections considered in this work. Followed is the theoretical analysis of backreflection penalties which was developed by another member of our group. The experimental results of my research are discussed and analyzed, which includes experimental setup, characteristics of system components as well as the detailed analysis and comparison of experimental results in various WDM-PON configurations.

Chapter 4 concludes the thesis work by summarizing the main achievements and suggested future work.

CHAPTER 2 WAVELENGTH-DIVISION-MULTIPLEXING PASSIVE OPTICAL NETWORKS (WDM-PONs)

2.1 Background overview

Today more than ever before, the fast-growing demand of high bandwidth, driven by popular video-on-demand services and emerging applications such as online gaming, has motivated the development of new technologies to satisfy such demand. Fig. 2.1 shows forecast of the evolution of the global consumer internet traffic from 2011 to 2016 [25]. We could see that internet video streaming and downloads, together with internet video calling will grow to over 54 percent of all consumer internet traffic in 2016. Currently, voice, broadcasting, and data are delivered to subscribers in separate networks, that is, public-switched telephone networks (PSTNs), community antenna television (CATV) networks, and digital subscriber line (DSL). However, it is believed that the three separate services can be offered in an integrated form of triple-play service which is delivered by a single network. To provide the bandwidth required for triple-play service, access connections using optical fibers were promoted as optical fibers have the advantage of high bandwidth, low loss and low noise. Such system is referred to as fiber-to-the-x (FTTx) system, where "x" stands for "home (H)," "curb (C)," "premises (P)," "business (B)," etc., depending on how close the optical fiber is drawn with respect to the subscriber's location.

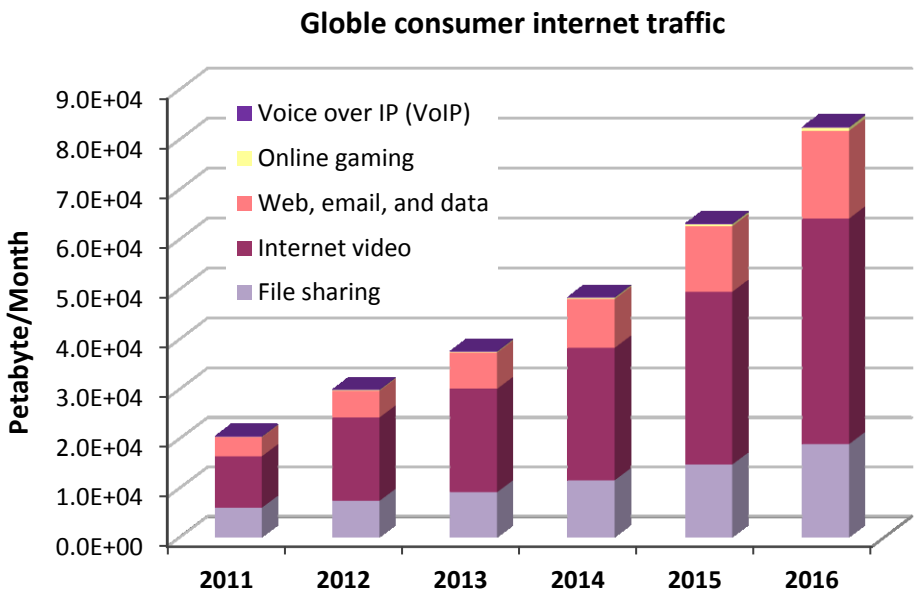

Fig. 2.1 Forecast of the global consumer internet traffic (2011-2016)

FTTH can be deployed using various architectures, as shown in Fig. 2.2. The home run in Fig. 2.2 (a) means P2P fiber connection between the CO and a home, which is expensive to install and handle the numerous fibers. To reduce the installation related costs, P2MP architectures were investigated as shown in Fig. 2.2 (b), where many subscribers share one fiber line through the remote node (RN). The RN performs function of active switching (Ethernet switch), or passive power splitting, or wavelength (de)multiplexing. Among them, the PON, which is a P2MP optical network with a passive RN, is preferred in terms of installation, operation, and maintenance of network. In a PON, there are no active elements in the signal path from source to destination. All transmissions are performed between an OLT at the CO and ONUs mainly through an optical splitter/combiner at the RN. PON has the ability to transport large amounts of data and information at very high bit rates through optical fiber as transmission medium in both feeder and distribution networks (called feeder fiber and drop fiber, respectively). PON-

based FTTH has been widely deployed in recent years. The total number of FTTH subscribers worldwide has grown to about 38 million at the end of 2011 and is expected to reach about 90 million at the end of 2015, representing about 15% of all subscribers [26].

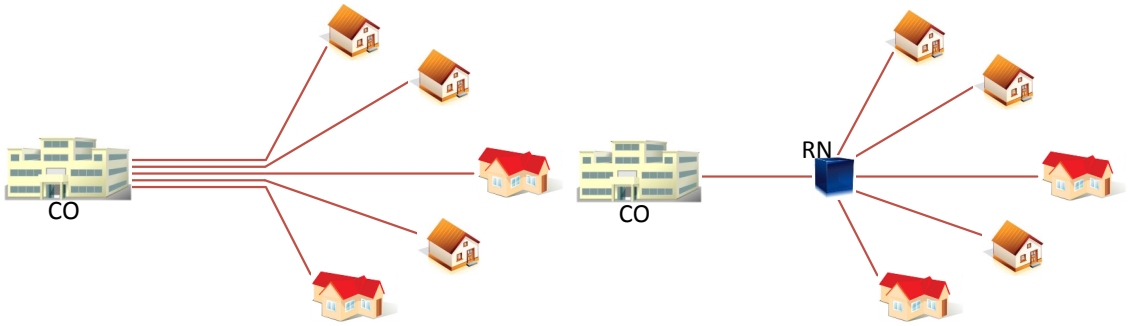

(a) P2P architecture (home-run) (b) P2MP architecture

Fig. 2.2 Various architectures of FTTH

At present, most of PON deployments utilize time division multiplexing (TDM) technique, in which dedicated time slots are assigned to each subscriber connected to the PON. However, most agree that TDM-PONs cannot cope with the requirements of future network evolution with respect to aggregated bandwidth and the allowable power budget [1-6]. These problems can be mitigated with WDM-PONs, in which ONUs are assigned individual wavelengths such that the bandwidth of fiber is utilized more effectively to further increase the transmission speed. The architectures for WDM-PONs have been proposed as early as the mid-1990s. However, its deployment has been delayed early days mainly due to lack of services and the high cost of the WDM components. As the bandwidth-intensive network applications continue to emerge, WDM-PON is beginning

to attract significant attention. Recently, substantial research efforts have been dedicated to find solutions for realizing cost-effective WDM-PONs.

2.2 PON architectures and standards

2.2.1 TDM-PONs

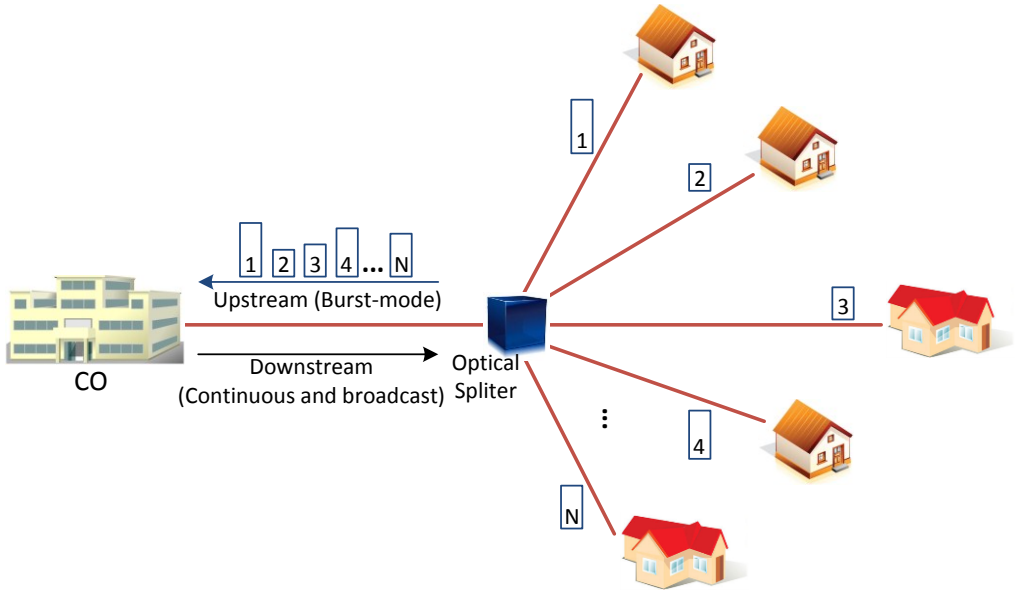

Fig. 2.3 Architecture of TDM-PON

TDM-PON is the most common commercial PON architecture. The transmission time is divided into discrete slots and each subscriber is granted access to the medium during a specific time slot, as depicted in Fig. 2.3. In the downstream direction, the OLT at the CO broadcasts the traffic through a passive optical power splitter at the RN to all ONUs in the access network and accordingly, all broadcasted information is received by every ONU. The data streams for different ONUs can be virtually differentiated using ONU address labels that are embedded in the transmission. At the ONU, only the relevant data

with correct address labels is processed and other data is discarded. The upstream signals are coupled through the same power splitter. TDM is employed in order to avoid the collisions between transmissions of different ONUs' in the network. Variable length transmission time slots can be assigned for each ONU depending on the required quality of service. This mechanism is commonly known as dynamic bandwidth allocation and is managed by the OLT.

However, TDM-PON suffers from several disadvantages [2, 3], [27]:

- Bandwidth sharing: the bandwidth per ONU is limited.
- The splitting ratio introduced by the passive splitter that limits:
    - the maximum number of ONUs in a PON,
    - the maximum reach of a PON,
- Security issue: security algorithms for downstream signals are required because the downstream information is going to every ONU.
- Complicated bandwidth allocation protocol.

2.2.2 WDM-PONs

WDM-PON provides the dedicated bandwidth of a P2P network with the fiber sharing inherent in PON access networks. The straightforward approach to build a WDM-PON is to employ a separate wavelength channel from the OLT to each ONU, as shown in Fig. 2.4. In the downstream direction, the wavelength channels are routed to the corresponding ONUs using a passive arrayed waveguide grating (AWG) as a WDM demultiplexer, which is deployed at the RN. The AWG replaces the passive power

splitter used in a TDM-PON. The AWG is a passive optical device with the special property of periodicity, the cyclic nature by which multiple wavelength channels are routed to the same output port from an input port. This enables spatial reuse of the wavelength channels. The insertion loss does not scale with the number of users and is considerably smaller than a passive splitter and (for example a 1x32 splitter introduces loss of 18 dB while the loss of AWG is typically in the range of 3-5 dB, independently of the number of routed channels). For the upstream direction of the WDM-PON, the same AWG performs as a WDM multiplexer to combine all the upstream wavelength channels together. At the OLT, another AWG is employed along with a receiver array to detect the upstream signals. In such WDM-PON architecture, each subscriber gets a dedicated P2P optical channel to the OLT, although they are sharing a common P2MP physical architecture like the TDM-PON.

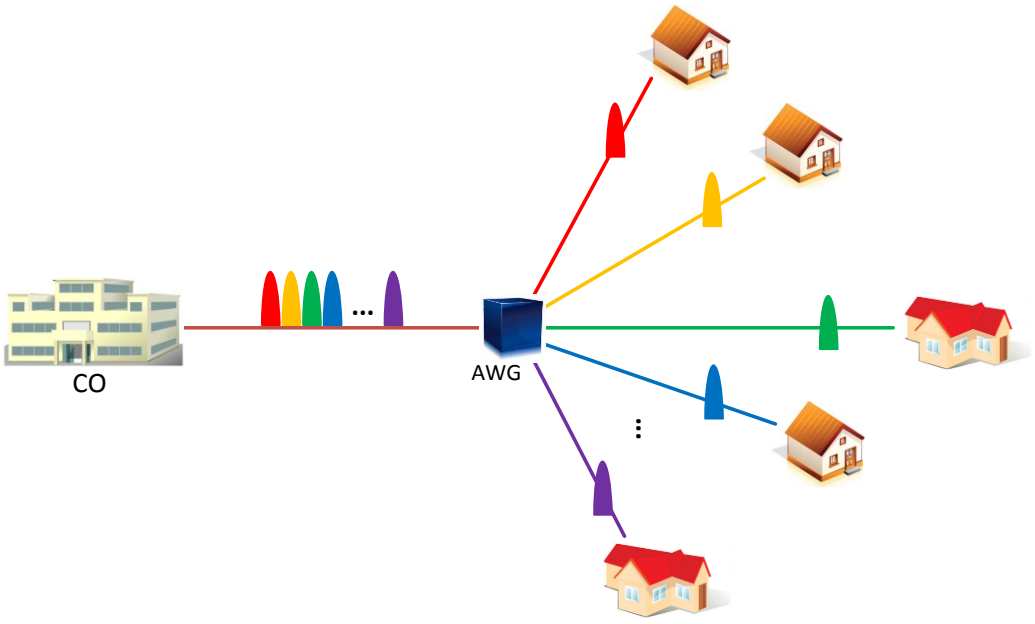

Fig. 2.4 Architecture of a WDM-PON

Because of the virtual P2P architecture of WDM-PON, it has many advantages over the TDM-PON [2, 3]:

- Huge bandwidth: each ONU is assigned an individual wavelength which provides inherent advantages in terms of bandwidth per ONU (each user can operate at a rate up to the full bit rate of a wavelength channel).
- The usage of the AWG router removes the splitting loss problem increasing the reach and scalability.
- Good security and protocol transparency: no sharing information between users.
- Less complexity and easier implementation: no need for any sophisticated media access controller algorithms to manage the timing of the ONU transmissions.

Although a WDM-PON has many technical advantages, there have been several issues that have prevented it from being a suitable solution for access applications. One issue has been related to the polarization independence and the wavelength stability of the AWG at the RN. AWGs usually require thermal control to keep their wavelength channels locked to the International Telecommunication Union (ITU) grid. This requires active electrical control at the RN which is not acceptable for a passive solution. Technology advances have allowed the recent commercialization of athermal AWGs that can remain locked to a dense WDM (DWDM) wavelength grid over temperature ranges experienced at the passive-node location [28]. Another issue is the concern of using wavelength-specific sources in the WDM-PON system. Such sources would require thermo-electric coolers to stabilize their wavelengths. Wavelength stabilized lasers are usually expensive. In addition, this scheme would require a different or "colored" transceiver for each user, resulting in high costs for installation, management,

maintenance and inventory. For the practical realization and deployment of the WDM-PON access networks, technologies to reduce the system cost needs to be developed.

2.2.3 PON standards

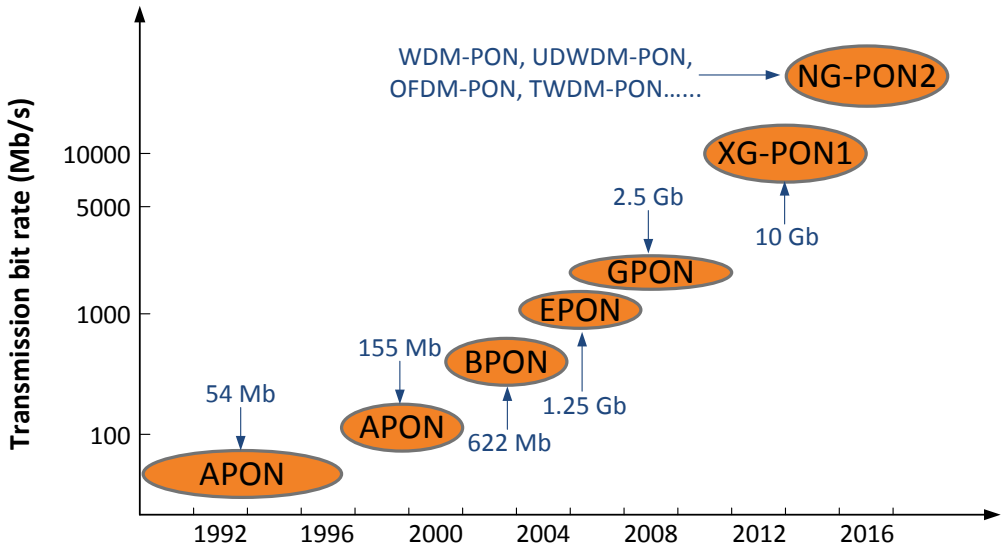

Fig. 2.5 Evolution of PON standards (modified from [3])

Many TDM-PON standards have been established, such as asynchronous transfer mode PON (APON) [29, 30], broadband PON (BPON) [31], Ethernet PON (EPON) [32], and Gigabit PON (GPON) [33]. The next-generation GPON standard, which is classified as XG-PON1, has been released in 2010 [34, 35]. A number of options have been considered for next generation broadband access standard (NG-PON2), This includes WDM-PON, coherent ultra-dense WDM-PON (UDWDM-PON), orthogonal frequency division multiplexing (OFDM) PON, and TWDM-PON (TDM/WDM-PON), a hybrid system that stacks four 10GPONs onto a single fiber to deliver 40 Gb/s capacity

downstream, etc.. The evolution of PON standards is illustrated in Fig. 2.5. The increase of transmission bandwidth can be seen in the figure as the PON standard develops.

2.3 WDM-PON technologies

2.3.1 State of the art

The first country to deploy WDM-PON systems was South Korea and it had more than 100,000 lines by February 2007 [4]. Although wider scale deployment is technically feasible, the high cost of existing optical components has made such systems less attractive for implementation. The enterprise market has already had several WDM-PON vendors such as ADVA Optical Networking, Transmode and LG-Ericsson, and WDM-PON system has been commercialized. However, for instance, the cost of the WDM-PON developed by LG-Ericsson is roughly twice that of EPON or GPON [36]. Efforts toward standardization of the WDM-PON architecture have also started in the second half of 2010 for its practical deployment in the future [36].

DWDM, which offers a typical 100 GHz channel spacing, is commonly used in the long-haul and metro markets, but it has not yet been applied significantly in the access area mainly due to cost. One reason for this is the requirement that each remote site would need a unique transceiver (using a wavelength stabilized optical source) that is matched to the WDM channel defined by the optical transport layer. The need for differently "colored" transceivers has been a significant barrier for wide-scale WDM-PON implementation, due to the high operational costs (installation, maintenance, and

inventory) associated with managing each remote access location. Fixed lasers at different wavelengths have been proposed, as have also wavelength tunable lasers for implementing wavelength-adaptive (so called “colorless”) transmitters, but these are currently too expensive for FTTH applications. To address this issue, a lot of effort has been put in trying to develop low-cost sources that are “color-free” or “colorless” so that all subscribers can have identical ONUs. A lot of colorless architectures in WDM-PONs have been proposed, such as spectral slicing, injection and self-injection locking of FP-LDs, wavelength-seeding and self-seeding of RSOAs, etc.. To further reduce the cost, wavelength-reused technique, so called remodulation scheme, has also been proposed. The most popular and cost-effective architectures will be discussed in detail in following sections.

2.3.2 Colorless architectures in WDM-PONs

2.3.2.1 Injection-locking of FP-LDs

To reduce the cost of WDM-PONs, injection-locking scheme has been developed. This technology eliminates the wavelength-specific sources and replaces them with low-cost identical FP-LDs. Fig. 2.6 illustrates a WDM-PON system with injection-locked FP-LDs by spectrum-sliced ASE source. Two broadband light sources (BLSs) at different bands (C- and L-band) are located at the CO for injection of broadband light into FP-LDs located at the CO and the ONUs. L-band (1581.3–1585.8 nm) and C-band (1548.9–1553.3 nm) are used for the downstream and upstream data transmissions, respectively [37].

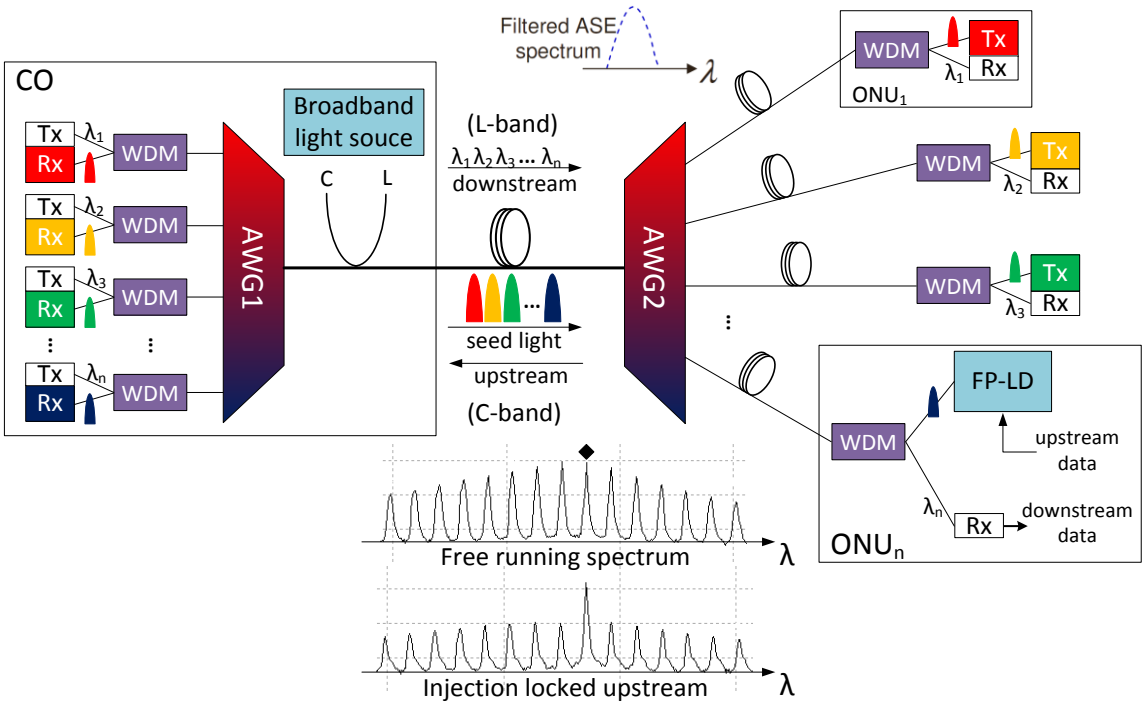

Fig. 2.6 A WDM-PON with injection-locked FP-LDs by spectrum-sliced ASE light

The ASE light from C-band BLS is coupled into the feeder fiber and sent to the AWG2 where it is spectrally sliced, and then injected into FP-LDs located at the ONUs. At the ONUs, the FP-LDs are directly modulated. When an external optical beam is injected into the cavity of a FP-LD, it experiences the internal gain from the semiconductor material. This process results in a reflected and amplified signal that contains the ONU data. Since the injected signal can be much larger than the internally generated spontaneous noise, the majority of the optical output power will be at the wavelength of the injected signal. The normal multi-wavelength spectrum of the FP-LD is transformed into a quasi single-wavelength spectrum similar to that of a DFB-LD. This narrowband output signal can then be efficiently transmitted through a DWDM communication channel. The externally injected wavelength is called the “locking” or “seeding” signal.

By maintaining the frequency of the seeding source sufficiently close to the FP-LD, the injection forces the FP-LD to operate only on the injected frequency with relatively little noise. After the injection-locking, the generated upstream signals are multiplexed by the AWG2 and transmitted through the feeder fiber back to the CO where the received signals are demultiplexed by the AWG1 and detected by the receivers. The upstream wavelength of each subscriber is determined by the wavelength of the injected spectrum-sliced BLS, since a mode of the FP-LD that is the nearest to the peak wavelength of the injected BLS is locked to the wavelength of the injected BLS. Therefore, although all the transmitters at the ONUs are identical, they operate at different DWDM wavelengths, making each ONU interchangeable which reduces management, installation and inventory costs. The injection locking can strongly improve the side-mode-suppression-ratio (SMSR) of a FP-LD, which is essential for DWDM operation.

For the downstream data transmission, L-band BLS output is coupled into the AWG1. It is spectrally sliced and injected into the FP-LDs located at the CO. The downstream signals are generated and then transmitted toward the user side and recovered by the receivers at the ONUs. The use of a separate upstream and downstream communication band is possible since the AWG is designed to be periodic in wavelength so it can operate in multiple bands. This means that an AWG can simultaneously support two communication wavelength bands on each of its input. The insets of Fig. 2.6 are examples of the spectrums of spectrum-sliced BLS, free-running FP-LD and injection-locked FP-LD, respectively. It is very clear that after the injection locking, the SMSR is improved dramatically.

The application of injection-locking of FP-LDs in WDM-PONs was first proposed in 2000, in which the spectrum-sliced ASE light was used as the seed light [11], and has been reported in several other studies [38], [39]. This scheme is very attractive due to its low cost and has been in use in Korea in the past few years [36]. However, since spectral slicing of a BLS inherently suffers from the conversion of excess intensity noise (EIN) from the seed light to the FP-LDs [40], [41] as well as incoherent characteristic, the transmission is typically limited to 1.25 Gb/s. An increased data rate of 2.5 Gb/s upstream transmission are achieved by injection-locking FP-LDs using a polarization insensitive supercontinuum pulse source [42], and by mutually side-mode injection-locking FP-LDs [43]. Recently, a demonstration of 2.5 Gb/s data rate with over 25 km transmission distance was achieved by using a MW-LS as the seed light. Certainly, if further increase of data rate is required, a high-quality coherent light source with low intensity noise such as DFB-LD needs to be utilized as the seed light at the current stage [44].

2.3.2.2 Wavelength-seeding of RSOAs

The idea of wavelength-seeding of RSOAs is similar to that of injection-locking of FP-LDs, with the FP-LD replaced by an RSOA. Compared to the injection-locked FP-LD, the wavelength-seeded RSOA has the advantage that it is immune to mode partition noise and wavelength selectivity, since the optical spectrum of the RSOA is a broadband one instead of a multimode one. Moreover, the EIN of the seed light can be suppressed by squeezing power fluctuation when the RSOA is operated in a gain saturation region [45].

And normally, there is no need to adjust the polarization of the seed light to maximize the gain.

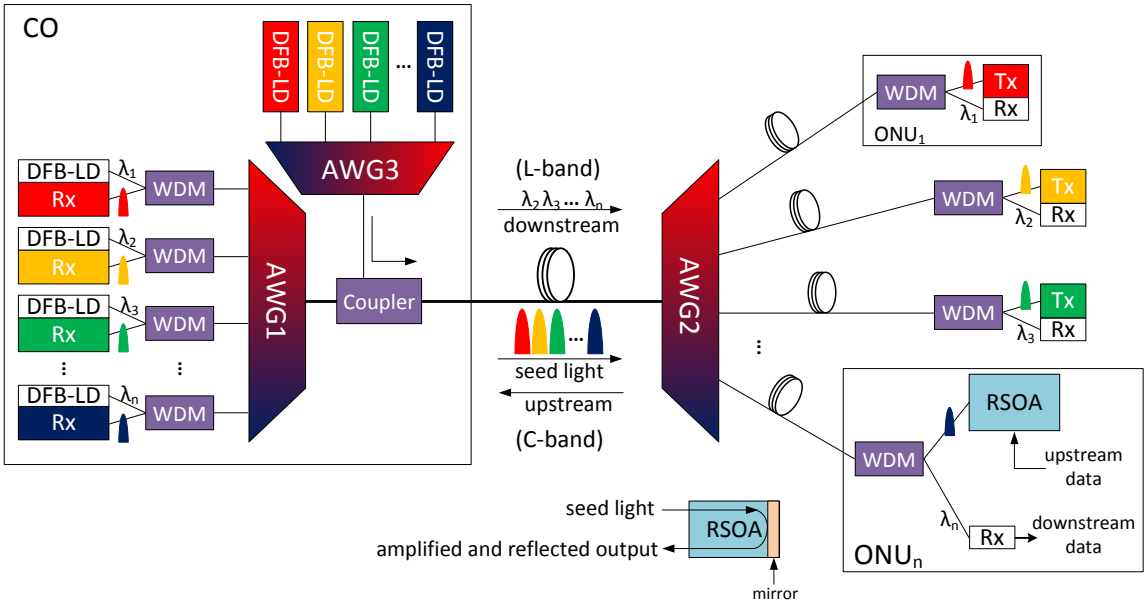

Fig. 2.7 A WDM-PON with wavelength-seeded RSOAs by coherent light

The architecture of the WDM-PON with wavelength-seeded RSOAs could be the same as that of injection-locked FP-LDs, except that the FP-LDs are replaced by RSOAs. As an example, Fig. 2.7 illustrates the architecture of a WDM-PON with wavelength-seeded RSOAs by a set of DFB-LDs. The use of coherent light as the seed light has the potential ability to decrease the ASE noise and increase the bit rate compared to the spectrum-sliced BLS, but more costly at the same time. The spectrums of the C-band DFB-LD array are multiplexed by AWG3 at the CO and coupled into the feeder fiber as the seed lights. At the RN, the seed lights are demultiplexed by AWG2 and transmitted toward each subscriber through the distribution fibers. The inset of Fig. 2.7 explains the mechanisms of the RSOA when the light is injected into it. By directly modulating the

RSOA, the amplified and reflected upstream signals are multiplexed by AWG2 at the RN, demultiplexed by AWG1 and detected by the receivers at the CO. The downstream signals are generated by directly modulating of an array of L-band DFB-LDs, which are multiplexed by AWG1 at the CO and coupled into the feeder fiber, demultiplexed by AWG2 at the RN, and detected by different receivers at subscribers' premises.

The first proposal of using wavelength-seeded RSOAs in WDM-PONs was reported in 2001, realizing a system with 1.25 Gb/s data rate over 25 km transmission [14]. Some other studies using the same technique have been demonstrated in [16], [46-48], but all of them are limited to 1.25 Gb/s data rate. Generally, RSOA modulation speed can be increased by high current injection and high optical power incidence. The former is restricted by power consumption at each CO/ONU, and the later by optical power budget in the WDM-PON. Afterwards, many investigations have been focusing on the techniques to increase the RSOA's bandwidth for higher transmission bit rate [49-52]. In [49], it shows the operation of RSOAs at 2.5 Gb/s of 20 km transmission thanks to the improvement in fabrication and packaging. In [51], it was demonstrated for the first time RSOA operation up to 5 Gb/s. Equalization techniques using RSOAs at 10 Gb/s have been shown at the expense of reduced receiver sensitivity and the need for forward error correction [53, 54].

2.3.3 Wavelength-reused remodulation schemes in WDM-PONs

A common characteristic in all the WDM-PON systems discussed so far is that they all use separate wavelength bands for the upstream and downstream transmission. This is to

reduce the crosstalk between signals and improve system performance. However, this means that in addition to the OLT light source required to carry the downstream data, an extra light source at the OLT is needed to seed the ONU. To realize more cost-effective WDM-PONs, remodulation schemes, in which the downstream optical signal is reused for the upstream transmission, have been investigated [9], [19-23]. The first remodulation scheme using injection-locked FP-LDs was proposed in [9]. In this system, the FP-LD located at the ONU was injection locked by a portion of the received optical power from the 10 Gb/s non-return-to-zero (NRZ) downstream wavelength and was simultaneously directly modulated to produce the upstream signal. Some remodulation schemes based on RSOAs have also been proposed [20-23].

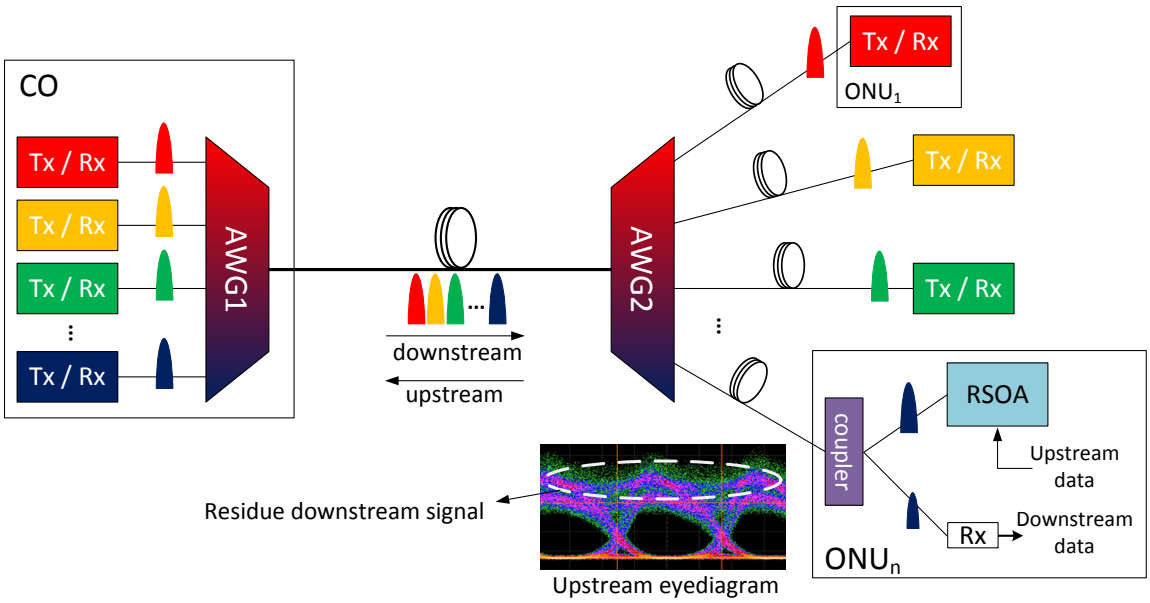

Fig. 2.8 Remodulation-based WDM-PON structure employing RSOAs

Fig. 2.8 shows the remodulation-based WDM-PON structure employing RSOAs. The downstream signals generated by transmitters in the CO are transmitted to the ONUs through AWG1 at the CO, the feeder fiber, and AWG2 at the RN. At each ONU, a

smaller portion of the downstream signal is detected by the receiver to recover the downstream data while the bigger portion is injected into the RSOA to be remodulated with the upstream data, and transmitted back to the receiver at the CO.

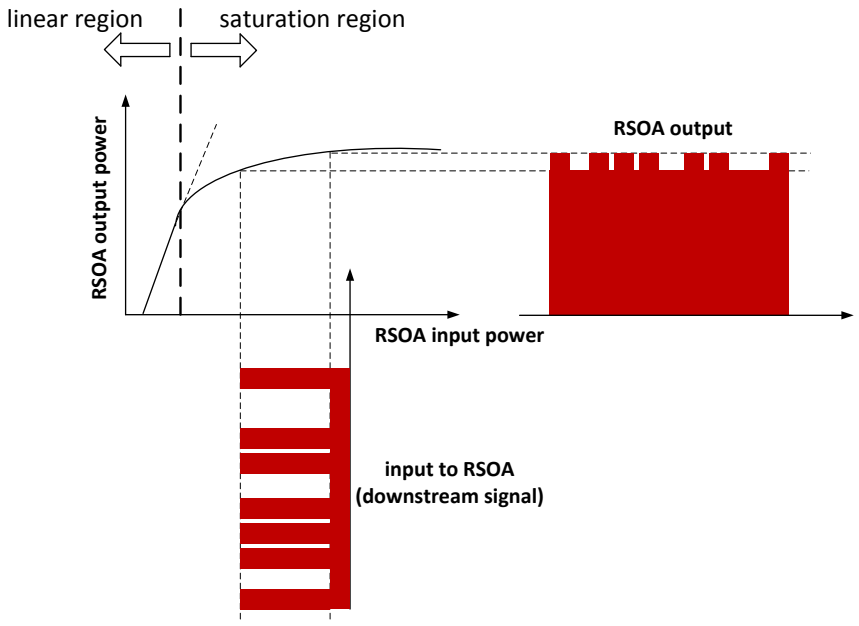

Fig. 2.9 Gain characteristic of the RSOA [55]

In these remodulation schemes, the RSOAs are operated in the gain saturation region so that the amplitude of the downstream signal can be suppressed. Fig. 2.9 shows the input–output characteristic of the RSOA, which indicates that the RSOA output power saturates as the input power (i.e., the downstream signal power) increases. The downstream signal is amplified by the linear amplifier so that its power is in the RSOA saturation region, and then injected into the RSOA. As a result, the difference between the mark and space levels is considerably reduced in the RSOA reflected output, which means that the downstream signal modulation pattern can be almost erased. At the same time, by

modulating the RSOA injection current with a different signal, the upstream signal with the same wavelength as the downstream signal is generated.

However, in such schemes, the residual downstream component included in the upstream signal can cause the performance degradation in upstream transmission, as shown in the inset of Fig. 2.8. Therefore, such schemes usually require high injection power and sacrifice the extinction ratio (ER) of the downstream data to reduce the crosstalk to the upstream signal. To overcome this disadvantage, it has been proposed to use subcarrier multiplexing together with WDM to separate frequency bands between upstream and downstream data [56–58]. It was also demonstrated that using different modulation formats for downstream and upstream helps in erasing the downstream pattern [19], [59-63]. However, these methods increase the complexity as well as the cost of the WDM-PON.

2.3.4 Comparison of various colorless architectures in WDM-PONs

In addition to the colorless architectures discussed above, more solutions are available. The most cost-effective solution would be the spectrum slicing scheme. In such system, the ONU uses a broadband light-emitting diode (LED) or semiconductor optical amplifier (SOA) to modulate upstream information, and then the AWG at the RN slices out the corresponding wavelength of each of the subscribers [64, 65]. The drawback is the optical power wasted in the slicing process which decreases the achievable reach. Moreover, the slicing process introduces intensity noise, which limits the bit rate.

The tunable laser approach would be the natural colorless solution. The device wavelength could be configured and this scheme offers a high degree of flexibility and performance (reach, bit rate, etc.). But no commercial WDM-PON solution based on tunable lasers is available due to their current high cost.

To reach modulation speeds of 10 Gb/s or even higher, the reflective electro-absorption modulator (REAM) offers a solution [66-68]. The cost is the main problem with such scheme. In addition, another drawback of this scheme is that the REAM lacks optical amplification meaning that twice the link-loss must be covered [36].

In contrast to injection-locking of FP-LDs and wavelength-seeding of RSOA, self-seeding technique has also been proposed to eliminate the use of centralized light source (CLS) as the seed light. In such a scheme, instead of a master device, the seed signal is taken from the FP-LD or RSOA itself. In the case of FP-LD, fiber Bragg gratings (FBGs) with pre-assigned Bragg wavelengths are implemented at the AWG ports to reflect light from FP-LDs for self-injection locking [69]. In the case of RSOA, broadband ASE light emitted from each RSOA is spectrally sliced by an AWG at the RN and fed back via a passive reflective path to seed itself [70, 71].

Table 2.1 concludes a comparison of the colorless architectures, including bit rate/channel, number of channels can be supported, as well as their own advantages and disadvantages. According to the table, the schemes discussed in sections 2.3.2 and 2.3.3 are more favorable in terms of both performance and system cost.

Table 2.1 Comparison of colorless architectures [72]

Scheme	Bit rate /channel	No. of channels	Pros	Cons
Spectrum slicing: LED	Low, <155 Mb/s	Low, ≤16	Very cheap No seed needed	Poor scalability and reach
Spectrum slicing: SLED/SOA	Low, <155 Mb/s	Medium, ~32	Inexpensive No seed needed	Low bit rate and short reach
Injection locked FP with ASE injection	Low, ~1.25Gb/s	Medium, ~32	Inexpensive	Non-standard FP needed (wide gain spectrum) Bit rate and transmission distance limited
Injection locked FP with laser injection	Medium, >2.5Gb/s	Medium, ~32	Inexpensive	Non-standard FP needed (wide gain spectrum) Polarization dependent upon injection
Injection locked FP with self-seeding	Medium, >1.25Gb/s	Medium, ~32	Inexpensive No seed needed	Non-standard FP needed (wide gain spectrum) Polarization dependent upon injection
RSOA: with ASE injection	Medium, <5Gb/s	Medium, ~32	Relatively high bit rate	Relatively expensive, Seed source needed Chromatic dispersion limited
RSOA: laser array seeding	Medium, <5Gb/s	High, >32	Relatively high bit rate	Laser bank seed source needed, Polarization dependent, backscattering problem
RSOA with remodulation	Medium, <5Gb/s	High, >32	Relatively high bit rate, No seed source	Downstream extinction ratio is limited Backscattering affects upstream performance
REAM	High, >10 Gbit/s	Low, <32	High bit rate	Expensive; Relatively high injection power Backscatter affects upstream performance
Tuneable laser	High, ≥10Gbit/s	High, ≥32	Good output power => long reach No seed needed Wavelength flexible	Expensive External modulator needed Wavelength assignment algorithm needed

2.4 Impairments in single-fiber bidirectional WDM-PONs

Various desirable architectures of WDM-PONs have been discussed. In all of these systems, one single fiber is deployed between the CO and the RN for transmission of both downstream and upstream signals. Single-fiber transmission presents a very efficient solution because only one fiber is necessary, and at the same time, the cost for connectors, splices and other network components decrease as well. Such single-fiber bidirectional transmission can be implemented using two strategies, which is illustrated in Fig. 2.10. The one in Fig. 2.10 (a) represents the one which is to transmit downstream and upstream data using different wavelength so that the signals do not interfere with each other. This

option requires sources of different wavelength as well as WDM couplers to divide the downstream and upstream channels. The second alternative is shown in Fig. 2.10 (b) in which the same wavelength is used in both directions. In this configuration, the savings of fiber and wavelength brings the most cost-effective solution. However, the crosstalk and interference between the signals results in more noise which may lead to a poorer performance.

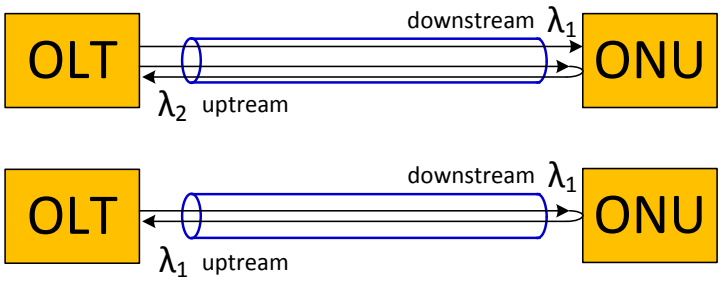

Fig. 2.10 Options for single-fiber bidirectional transmission: (a) one fiber with two wavelengths; (b) one fiber with one wavelength

A typical implementation of the schemes shown in Fig. 2.10 (a) would be the colorless ONU architectures such as injection-locking of FP-LDs or wavelength-seeding of RSOAs. For example, as reported in [37] (Fig. 2.6), C-band signals are transmitted from the OLT to the ONU, and after injection-locking of FP-LDs, are sent back to the OLT as the upstream signals. On the other hand, L-band signals are transmitted from the OLT and detected at the ONUs as the downstream signals. For the scheme shown in Fig. 2.10 (b), wavelength-reused remodulation technique would be a good example. In such scheme, there is no need for additional seed light, instead, the downstream itself is the seed light and is reused to generate the upstream signal with the same wavelength. These two

schemes are both single-fiber bidirectional WDM-PONs and the impairments in such schemes are discussed in the following sections.

2.4.1 Fiber loss

Fiber loss is a major factor that limits the transmission distance in optical communication systems due to the inherent characteristic of the optical fiber. In fact, the use of silica fibers for optical communications became practical during the 1970s, only when losses were reduced to an acceptable level [73]. As the signal power is reduced gradually along the transmission direction, the detected signal power at the optical receiver could be too low to be recovered accurately since a certain minimum amount of power is required for accurate detection. With the advent of optical amplifiers in the 1990s, transmission distances can exceed several thousands of kilometers by compensating accumulated losses periodically.

The fiber loss depends on the wavelength of transmitted light. For the standard single-mode fiber (SMF), in the wavelength region near 1.55 μm, the fiber exhibits a loss of about 0.2 dB/km. This value is close to the fundamental limit of about 0.16 dB/km for silica fibers.

Nowadays, in addition to higher bit rates, another significant trend in PON research has been toward longer reach PONs, which normally can be realized by deploying more active amplifiers. However, considering the cost of practical PON system, the better solution would be to develop low-loss optical fibers. In 2009, Corning Inc. demonstrated a system that use an ultra-low-loss fiber with up to 3 dB lower loss over a 100 km system

length than standard SMF, thus enabling a split over twice as many subscribers [74]. Today Corning's advanced low-loss fiber manufacturing technology delivers enhanced single-mode ITU-G.652.D compliant optical fiber with a significantly reduced attenuation coefficient across the entire operational wavelength spectrum, i.e. from 1260 nm to 1625 nm. Corning's SMF-28® ULL optical fiber has demonstrated the lowest loss of SMF with maximum attenuation available between 0.17 and 0.18 dB/km at 1550 nm [75].

Low-loss optical fiber delivers improved link power budget, thereby enabling increased subscriber coverage, extended CO coverage to allow consolidation of redundant facilities, higher PON splitter ratios, and migration and coexistence of different system generations operating on the same fiber.

2.4.2 Fiber dispersion

Fiber dispersion is an important design issue in optical communication systems, especially in high-bit-rate systems. Basically, fiber dispersion leads to broadening of individual optical pulses with propagation. If optical pulses spread significantly outside their allocated bit slot, the transmitted signal is severely degraded. Eventually, it becomes impossible to recover the original signal with high accuracy. Hence, there is a limitation of bit rate-distance product brought by the dispersion, which can be expressed as [73]

$$BL|D|\Delta\lambda \leq 1 \tag{2.1}$$

where B represents the bit rate, L is the fiber length (transmission distance), D denotes the fiber dispersion coefficient, and $\Delta\lambda$ is the spectral width of the transmitted signal.

According to this formula, the signal with small spectral width is preferred to increase the bit rate-distance product; in other words, the signal from a BLS would not be a good choice for optical communication systems. However, in WDM-PON access networks, the spectrum-sliced BLS seeded optical sources, such as an injection-locked FP-LD and a wavelength-seeded RSOA by a spectrum-sliced ASE source like an erbium doped fiber amplifiers (EDFA), have been considered as attractive solutions for cost-effective implementation of high-capacity WDM-PONs, as discussed earlier. Even though the spectrum slicing process narrows the spectrum width of a BLS because of the AWG or the filter, the bandwidth is still wide compared to other laser sources such as the DFB-LDs. Hence, in such systems, the system's performance is severely degraded by the dispersion of transmission fiber [76-78]. The chromatic dispersion could increase not only the inter-symbol interference due to the signal pulse broadening, but also the EIN suppressed within the FP-LD or RSOA [76, 77]. A dispersion penalty equation has been reported in [78] to estimate the system's penalty in the WDM-PON using injection-locked FP-LDs by the BLS. It has been demonstrated that fiber dispersion is not a limiting factor for WDM-PONs with injection-locked FP-LDs running at 1.25 Gb/s or 2.5 Gb/s, because a well-locked FP-LD operates in a single mode and its linewidth is about 0.1nm [79]. In a very recent study [80], it shows that the effect of dispersion-induced EIN increase could be mitigated with an enough BLS seed source power into the RSOA. In this way, the maximum reach in a wavelength-seeded RSOA based WDM-PON

operating at a 1.25 Gb/s could be increased to be > 60 km of conventional SMF without using any dispersion compensating techniques.

2.4.3 Intensity noise from BLS and colorless ONUs

The incoherent spectrum-sliced BLS has been considered as an attractive candidate of WDM-PON light sources as it capitalizes on the economical advantages of generating multichannel lights simultaneously. However, these sources have thermal-like properties since they emit light through spontaneous emission and consequently have EIN which is a major limiting factor in transmitting data at a required bit rate and distance. At high bit rates, with correspondingly large receiver bandwidths, the detected EIN becomes significant, requiring an increase in receiver power to maintain a similar bit error rate (BER) that would be obtained when using a source relatively free from such noise, like a laser.

To address this limitation of incoherent sources, a number of techniques to suppress the EIN have been investigated. An all-optical method using intra-channel four-wave mixing (FWM) has been demonstrated to reduce the EIN by significantly increasing the received channel bandwidth [81]. Recently, it has been reported that the gain saturation characteristics of FP-LD or RSOA could significantly suppress the EIN within a spectrum-sliced BLS output, and thus improve the performance of BLS based WDM-PONs [82, 83]. Low-noise BLS based on mutually injected FP-LDs has also been proposed in [84, 85].

Moreover, in WDM-PONs, there are other sources of intensity noise. The spectral filtering by multiplexer/demultiplexer results in an increase in EIN. The increased EIN restricts data bandwidth when the spontaneous–spontaneous beat noise becomes dominant in the optical receiver. It has been demonstrated that a spectrum-sliced WDM-PON design by using flat-top passband AWGs as well as a narrow-bandwidth seed light source, to reduce the multiple spectral filtering effects at the multiplexers of the OLT and the RN [86]. The ASE noise from RSOAs, the intensity noise and mode partition noise from injection-locked FP-LDs, all contributes to the degradation of system performance in WDM-PONs.

2.4.4 Rayleigh backscattering (RB)

As we know, the two main loss mechanisms in an optical fiber are material absorption and Rayleigh scattering. Material absorption includes absorption by silica as well as the impurities in the fiber. The loss due to material absorption has now been reduced to negligible levels at the wavelengths of interest for optical communication-so much so that the loss due to Rayleigh scattering is the dominant component in today's fibers.

Rayleigh scattering arises because of fluctuations in the density of the medium (silica) at the microscopic level. The loss due to Rayleigh scattering is a fundamental one and decreases with increasing wavelength. The loss coefficient α_S due to Rayleigh scattering at a wavelength λ can be written as [87]

$$\alpha_S = A / \lambda^4 \tag{2.2}$$

where A is called the Rayleigh scattering coefficient. Note that the Rayleigh scattering loss decreases rapidly with increasing wavelength due to the λ^{-4} dependence. α_S represents the portion of the incident power scattered due to Rayleigh effect for length unit [m^{-1}].

When an optical pulse of peak power P_0 is injected into an optical fiber, the Rayleigh backscattered power observed at the input fiber end face from a distance z can be expressed as [88]

$$P_b = \left(P_0 S \alpha_S \Delta z\right) \exp\left(-2\alpha z\right) \tag{2.3}$$

where the capture fraction S is defined as the proportion of the total power scattered at z which is recaptured by the fiber in the return direction. Δz is the pulse travel distance element.

In single-fiber bidirectional WDM-PONs, as depicted in Fig. 2.10, there is beat noise caused by the Rayleigh backscattering (RB). In the system shown in Fig. 2.10 (a), even though the downstream and upstream signals are assigned with different wavelength, the seed light which has the same wavelength as the upstream signal goes from the OLT to the ONU, so that the backscattered seed light beats with the upstream signal which leads to the degradation of the upstream transmission. The impact of the beat noise on the system shown in Fig. 2.10 (b) is even worse. In this case, the upstream signal beats with the backscattered downstream signal and the downstream signal beats with the

backscattered upstream signal as well, which results in the worse performance for both signals.

As the RB is an intrinsic phenomenon in optical fibers and can not be eliminated, a number of studies have been reported to reduce the impact of RB in WDM-PONs [89-96]. A technique, using a phase modulator at the ONU to reshape the spectrum of the upstream signal in order to reduce the overlap with the backreflected light and hence to reduce the beat noise falling within the receiver bandwidth, has been shown in [89]. The RB reduction by means of optical frequency dithering has been presented in [90, 91]. In [90], the optical frequency modulation was realized by applying a pilot signal to a tunable laser, adequately adjusting the amplitude, frequency, and waveform of the pilot. In [91], by adjusting the dithering frequency of the downstream transmitter at the OLT using a simple feedback control, the reflection-induced penalties are suppressed drastically, for both the upstream and downstream signals. The technique for RB noise compression by using gain-saturated SOA has been demonstrated in [92]. The scheme enabled error-free, 10 Gb/s transmission to be achieved in a 64 way-split, 20 km reach WDM-PON. Moreover, in [93], by employing an RSOA as the ONU transmitter and driving it by a return-to-zero (RZ) signal, the coherence time of the upstream signal can be dramatically reduced. This technique increases the tolerance to the in-band crosstalk caused by RB up to 10 dB of signal-to-crosstalk ratio. An approach based on the use of line coding and proper electrical filtering has been introduced, in which an increased tolerance to the signal-to-crosstalk ratio by about 5 dB was achieved [94]. RB mitigation by FWM-assisted wavelength shifting has been demonstrated and tested in an extended reach PON [95]. Full-duplex 10/2.5 Gb/s transmission has been validated over long reach > 50 km

and a high tree split of 1:32. In [96], a seeding source which comprised of conventional DFB-LD with intentional optical feedback has been proposed for the reduction of RB induced power penalty.

2.5 Summary

In this chapter, an overview of WDM-PON technologies has been provided. Section 2.1 gives the historical background of the development of WDM-PONs. It demonstrates that access network has been developed from traditional copper wire towards PON-based FTTH because of the fast-growing demand for higher bandwidth. Even though the TDM-PON is the most popular PON architectures, WDM-PON is believed to be the ultimate solution for higher bandwidth. In section 2.2, the evolution of PONs is introduced, including the basic concept of FTTH access networks, the two main architectures of PONs, i.e., TDM-PONs and WDM-PONs, and various PON standards. A number of advantages of WDM-PON over TDM-PON are discussed. Section 2.3 focuses on the main challenges and technologies in the deployment of WDM-PON access networks. The recent technologies developed to realize wavelength-independent, so-called colorless, architectures are very attractive low-cost solutions for WDM-PONs. The most popular colorless architectures in WDM-PONs, such as injection-locking of FP-LDs, wavelength-seeding of RSOAs and wavelength-reused remodulation schemes, are described and compared. Finally in section 2.4, the main impairments in single-fiber bidirectional WDM-PONs are described, such as fiber loss, fiber dispersion, intensity noise from BLS and colorless ONUs, and RB. Some of the technologies to overcome these impairments

are also discussed. As an inevitable factor in optical fibers, it has been shown that it is very important to investigate the impact of backreflections on single-fiber bidirectional WDM-PONs.

CHAPTER 3 INVESTIGATION OF BACKREFLECTIONS IN SINGLE-FIBER BIDIRECTIONAL WDM-PONs

3.1 Motivation

As discussed in Chapter 2, in a single-fiber loopback optical communication system, bidirectional transmission results in beat noises between backreflections and the signal, which leads to degradation of the system performance. The backreflections include Rayleigh backscattering (RB) from the fundamental properties of the optical fiber as well as the Fresnel reflection from the components and the connectors. Recently, a number of papers have studied the impact of backreflections on single-fiber loopback access networks [97-112] and a few methods to mitigate this detrimental effect have been proposed [89-96]. Among those papers, [97-102] investigated the penalties caused by RB in a single-fiber bidirectional system. [103-110] analyzed the impact of backreflections specifically in WDM-PON access networks, in which the RB effects have been discussed in [103-108], and the impact of an external or a discrete reflection has been investigated in [104], [108-110]. In [111, 112], the noise due to double RB has been analyzed, which is particularly useful in long-haul amplified transmission systems where many amplifiers are cascaded.

In [103], the performance of PONs using centralized light sources (CLSs) impaired by interferometric noise has been analyzed. The effect of the noise generated by RB was

theoretically investigated, taking into account the modulation spectra of high bit rate signals. The impact of in-band crosstalk on the system's performance in wavelength-locked FP-LD-based WDM-PONs was investigated in [104]. It was shown that the wavelength-locked FP-LD injected by using an incoherent BLS is more tolerant to in-band crosstalk than DFB-LD. In addition, [105] and [106] demonstrated that there is an optimum ONU gain to minimize the backreflection impact on the upstream transmission in single-fiber WDM-PON access networks. In [105], an intensity noise estimation scheme was presented to estimate the impact of RB. It showed that the ONU gain must be optimized to maximize the SNR. The optimum ONU gain is dictated by the TLL. In addition, other than the TLL, the multiplexer's position was taken into account as well in [106]. It demonstrated that the best crosstalk-to-signal ratio is achieved if the multiplexer is placed either in the ONU or OLT vicinity, and the ONU gain has a new optimum value depending on the multiplexer's position. In this case, the optimum ONU gain is decided by the TTL as well as the position of the multiplexer. However, in a real-world deployment, the position of the multiplexer is usually determined by more practical considerations, like the cost, the physical distribution of the customers, etc. The same idea was utilized in [107], where the effects of RB in a long-reach RSOA-based WDM-PON operating at 1.25 Gb/s were investigated. In this network, a remote EDFA was assumed to be used at the RN. The penalty induced by RB was evaluated experimentally as a function of the EDFA gain for various lengths of drop fibers. It showed that the penalty is dependent on the EDFA gain and there is an optimum EDFA gain to minimize this penalty. The optimum EDFA gain depends highly on the length of the drop fiber. In all of the above papers [103-108], the impact of RB in a single-fiber bidirectional WDM-

PON access network were discussed. However, all of these analyses are only valid in a specific scheme and cannot be applied to all of the WDM-PON configurations with colorless ONUs. For instance, [104] applies to injection-locked FP-LD-based WDM-PONs, and [107] applies to long-reach wavelength-seeded RSOA-based WDM-PONs. As shown in Chapter 2, during the development of WDM-PON, various wavelength-independent ONU candidates, such as FP-LDs and RSOAs, have been applied in the network to reduce the costs of operation, administration and maintenance. The light source at the OLT, which is performed as the seed light of the ONU, could be different as well. Examples are a coherent light source like a DFB-LD, a spectrum-sliced broadband ASE source and a filtered MW-LS. Considering the different linewidth of the seed light and the chirp effect of the modulator at the ONU, the impairments of RB are different. Hence, it is important to take them into account and study the Rayleigh backreflection impact using various ONU and OLT configurations. Moreover, as discussed earlier in Chapter 2, there has also been significant interest in reutilizing the downstream signal as the seed light of colorless ONUs, which is known as the remodulation scheme [19-23], [59-63]. This configuration eliminates the need for an extra CW seed light which makes it more cost-effective. The remodulation technologies include various coding and modulation formats such as NRZ [20-23], inverse return-to-zero (IRZ) [62], Manchester coding [63], as well as advanced modulation formats such as DPSK [19], [59-61]. In such configurations, the ER of the downstream signal is an extra important parameter needs to be considered. None of the above papers has studied the impact of RB in WDM-PONs with remodulation scheme.

3.2 Principles of backreflections in WDM-PONs

3.2.1 Backreflections I & II

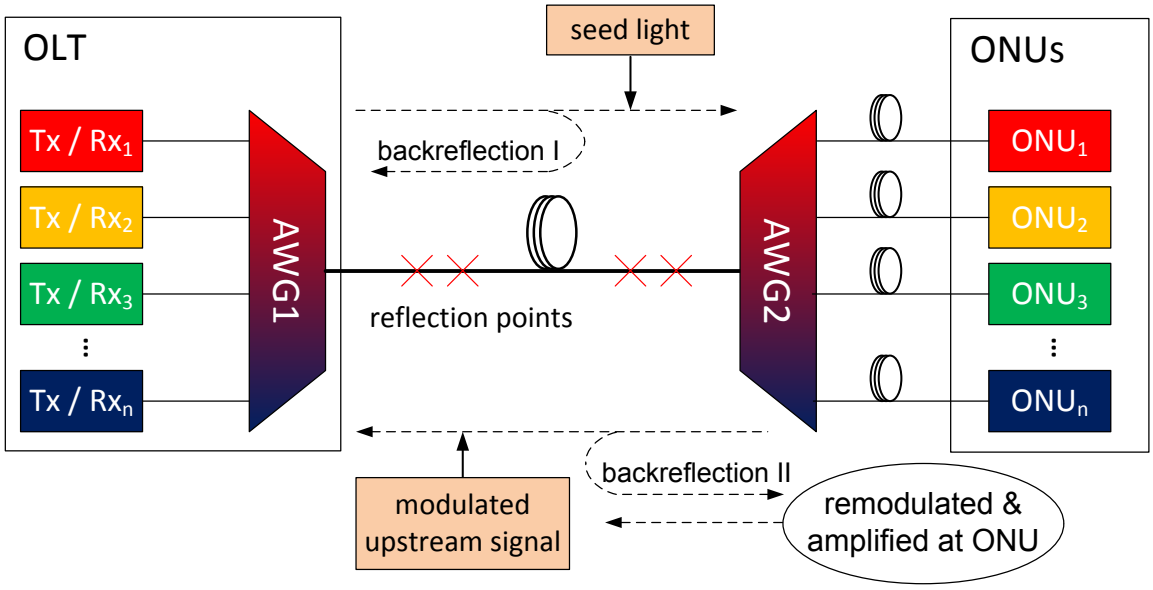

Fig. 3.1 Backreflections I and II in single-fiber bidirectional WDM-PON access network

In an actual access network system, reflection points from connectors and splices are presented, and RB exists even in a perfect optical fiber. In a single-fiber bidirectional WDM-PON access network, the backreflected up/down stream signal beats with its counter-propagating one (down/upstream) as both signals have the same wavelength and transmits in the same direction resulting in beat noise. Fig. 3.1 illustrates the two dominant sources of backreflections in such network system. One is the backreflection of the seed light from the OLT (backreflection I), and the other is the remodulated and reamplified backreflection of the upstream signal (backreflection II). As shown in Fig. 3.1, backreflection I transmits toward the OLT and causes the beat noise at the OLT receiver as it interferes with the upstream signal. In addition, backreflection II proceeds

toward the ONU together with the seed light distributed from the OLT. It is remodulated at the ONU and sent back to the OLT, which results in beat noise as well at the OLT receiver. Therefore, the upstream signal suffers from SNR degradation due to beat noises from the interference with backreflection lights. Other reflections, such as double RB, are insignificant so that their impact is ignored.

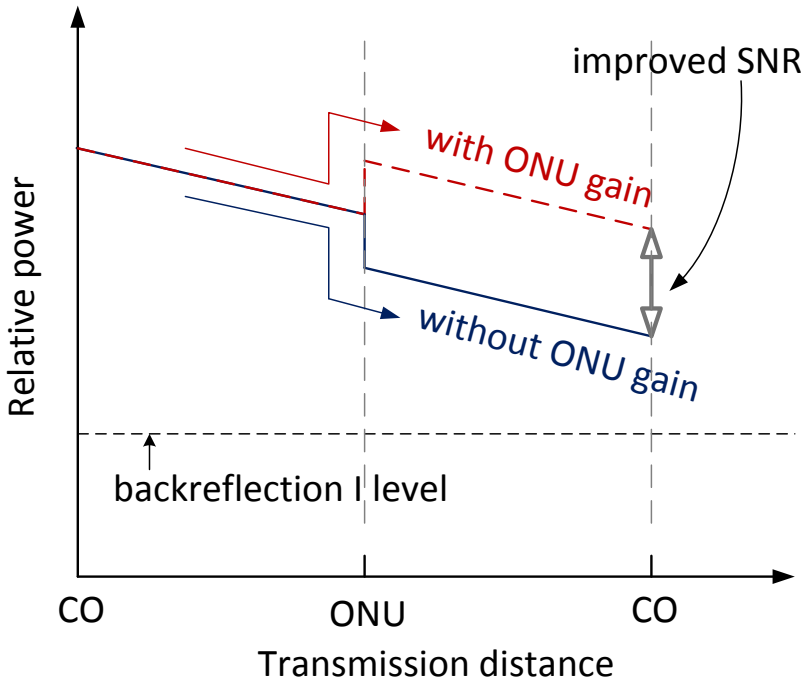

Fig. 3.2 Reducing the impact of backreflection I by signal amplification at ONU [105]

To reduce the beat noise caused by the interference, it has been proposed that the SNR degradation due to backreflections can be overcome by signal amplification at the ONU [101], [113]. Fig. 3.2 shows how this technique offsets the backreflection I and therefore reduces the impact of the beat noise. The vertical and horizontal axes (both are in decibel units) depict the upstream signal's relative optical power and its total transmission distance, respectively. As shown in the figure, since the signal power decreases with the

transmission distance, a relatively large signal to backreflection I power ratio cannot be achieved without signal amplification at the ONU. On the other hand, when there is signal amplification at the ONU, SNR can be improved as the signal power is increased against a constant backreflection I power. In this case, if only considering the impact of backreflection I, the higher the ONU gain the more improvement of SNR. However, in addition to backreflection I, the second type of backreflection, which is backreflection II, increases in proportion to the square of the ONU gain due to its double pass through the ONU. Hence, backreflection II has to be taken into account for the evaluation of the system performance.

Figure 3.3 illustrates the relationship between the intensity noise due to backreflections I, II and the ONU gain. In the figure, the vertical axis is the ratio of the backreflection power and the upstream signal power, while the horizontal axis is the ONU gain. We could consider the curves as the relative noise-to-signal ratio, in which case, the lower the better. The dotted curve shows that this ratio of backreflection I decreases linearly with the ONU gain because the power of backreflection I is independent of the ONU gain while that of the upstream signal increases linearly with the ONU gain. In contrast, the dashed curve shows that the ratio of backreflection II power and the upstream signal power increases linearly with the ONU gain as the power of backreflection II is proportional to the square of the ONU gain. As a result, the total noise-to-signal ratio, which is the combination of the dotted and dashed curves, is the solid curve. It is clearly shown that the noise due to backreflection I is dominant at low ONU gain. However, the impact of backreflection II exceeds that of backreflection I when the ONU gain is high.

Therefore, the optimum ONU gain is realized when the minimal total noise-to-signal ratio is achieved.

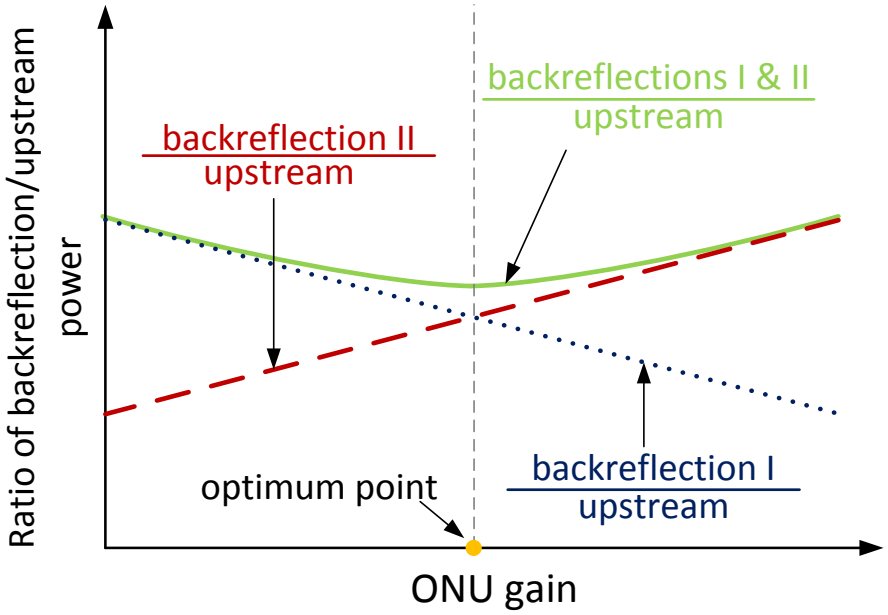

Fig. 3.3 Influence of ONU gain on SNR

3.2.2 Power penalty and optimum ONU gain

As discussed earlier, when both of backreflections I and II are taken into account, there is an optimum ONU gain to maximize SNR. In order to determine the value of the optimum ONU gain, the beat noises and power penalty caused by backreflections I and II needs to be calculated. In [105], by calculating the electrical field of the upstream signal and backreflection lights, and the relative intensity noise (RIN) on mark signals, the optimum ONU gain is derived by

$$G(dB) = TLL - 1.5 \tag{3.1}$$

However, there are other parameters that can not be ignored and need to be considered in the calculation. It is known that in fiber-optic transmission systems, the interference provides a mechanism for translation of laser phase fluctuations into receiver photocurrent fluctuations. As a result, the phase noise is converted to intensity noise through interference. In particular, the laser linewidth represents the laser phase fluctuations and is determined by the magnitude of the phase noise. Therefore, the interference of signals with different linewidths will cause different beat noise. In a single-fiber bidirectional WDM-PON access network, various seed lights from the OLT as well as different modulators at the ONU could be applied. Therefore, the interference between the signal and the corresponding backreflected signals is highly dependent on the linewidths of the beating signals and varies for different WDM-PON configurations. In addition, in most practical access networks, the modulator at the ONU is a chirped device so that the correlation between the seed light and the upstream signal is destroyed, which means that the seed light and the upstream signal are independent. Examples would be when a downstream signal is used for injection locking of a FP-LD, a VCESL or for seeding of a chirped RSOA at the ONU.

Therefore we present a general formulation for the impact of backreflections in WDM-PON access network, which includes the parameters mentioned above. The formulas were developed by another member in our group. In our analysis, both kinds of backreflections (backreflection I and II) are taken into account. Other reflections, such as double RB, are assumed insignificant. All backreflections are assumed to have the same polarization state as the upstream signal, which is the worst case as it results in maximum beat noise. If the polarization state of reflection is random, the beat noise will be half of

our presented results. The phase noise of the light source is considered to be a random variable with Gaussian probability distribution function [114]. In this derivation, we use integrals to represent continuous distributed reflection such as RB. However, the results are still valid as long as there are a large number of discrete reflection points. By calculating the electrical field of the upstream signal and that of the beat noises from backreflections I and II, the total optical power at the OLT receiver is derived. The power spectral density (PSD) could be obtained through Fourier transform of the autocorrelation of the photocurrent. As the photocurrent is in proportion to the optical power, the optical power's autocorrelation is calculated directly to obtain PSD. Hence, the RIN, which is the normalized PSD of the photocurrent relative to the signal, could be derived. Only the RIN at "one" state of the upstream needs to be calculated since the beat noise happens only at the "one" state. The detailed calculation process can be found in [115]. The following Equations (3.2) and (3.3) depict the distribution of RIN with the frequency f.

$$RIN_{dn} = \frac{2}{g\pi}\frac{R}{\alpha}\left(e^{2\alpha L}-1\right)\left[\frac{\Delta\nu_{d\_avg}}{\Delta\nu_{d\_avg}^2+\left(f-\Delta\nu_{d0}\right)^2}+\frac{\Delta\nu_{d\_avg}}{\Delta\nu_{d\_avg}^2+\left(f+\Delta\nu_{d0}\right)^2}\right] \tag{3.2}$$

$$RIN_{un} = \frac{g}{\pi}\frac{R}{\alpha}\left(1-e^{-2\alpha L}\right)\left[\frac{\Delta\nu_{u\_avg}}{\Delta\nu_{u\_avg}^2+\left(f-\Delta\nu_{u0}\right)^2}+\frac{\Delta\nu_{u\_avg}}{\Delta\nu_{u\_avg}^2+\left(f+\Delta\nu_{u0}\right)^2}\right] \tag{3.3}$$

where RIN_{dn} and RIN_{un} are RIN from backreflection I and II, respectively, g is the ONU gain which includes the component loss, α is the fiber attenuation, L is the fiber length, R is the reflection per unit length and is related to the ORL of the fiber by $R = ORL\cdot 2\alpha/\left(1-e^{-2\alpha L}\right)$, $\Delta\nu_{d\_avg}$ is the average linewidth of the upstream signal and

backreflection I, $\Delta\nu_{u\_avg}$ is the average linewidth of the upstream signal and backreflection II, $\Delta\nu_{d0}$ is the difference between the center frequency of the upstream and that of backreflection I, $\Delta\nu_{u0}$ is the difference between the center frequency of the upstream signal and that of backreflection II.

These expressions include the impact of the light source linewidth $\Delta\nu$ and the modulation bandwidth. The impact of the receiver bandwidth on the RIN is obtained by integrating the RIN with respect to frequency f over the frequency bandwidth of the receiver. Considering the RIN at "1" state of upstream data modulation, the power penalty, which results from the beat noises between the backreflections and the upstream signal, can be given by

$$\delta = -10\log_{10}\left(1 - Q^2 r^2\left(f_{bw}\right)\right) \tag{3.4}$$

where Q is the Q factor that represents the quality of the data transmission, f_{bw} is the receiver bandwidth and $r^2\left(f_{bw}\right)$ is the total RIN within this bandwidth. By differentiating in Eq. (3.4), the optimum ONU gain is obtained and can be shown as Eq. (3.5):

$$G(dB) = TLL + 1.5 + 5\log_{10}\left\{\frac{\int_0^{f_{bw}}\left[\frac{\Delta\nu_{d\_avg}}{\Delta\nu_{d\_avg}^2 + \left(f - \Delta\nu_{d0}\right)^2} + \frac{\Delta\nu_{d\_avg}}{\Delta\nu_{d\_avg}^2 + \left(f + \Delta\nu_{d0}\right)^2}\right]df}{\int_0^{f_{bw}}\left[\frac{\Delta\nu_{u\_avg}}{\Delta\nu_{u\_avg}^2 + \left(f - \Delta\nu_{u0}\right)^2} + \frac{\Delta\nu_{u\_avg}}{\Delta\nu_{u\_avg}^2 + \left(f + \Delta\nu_{u0}\right)^2}\right]df}\right\} \tag{3.5}$$

According to Eqs. (3.4) and (3.5), the RIN, power penalty and the optimum ONU gain are all related to the average linewidths of the upstream signal and backreflection I or II. For the ideal case, when the linewidth of the seed light is identical to that of the upstream signal, the optimum ONU gain formula can be simplified as

$$G(dB) = TLL + 1.5 \tag{3.6}$$

Compared with Eq. (3.1), this result is the same once the 3-dB modulation loss at the ONU is included. It tells us when the linewidth of the seed light and that of the upstream signal is the same, the optimum ONU gain depends only on the TLL between the OLT and the ONU. However, in practice, the colorless ONUs always have an impact on the linewidth of the seed light. For example, direct modulation of an RSOA results in chirp and broadens the linewidth. When the seed light is used for injection locking of a FP-LD, the linewidth of the upstream signal is impacted as well and is not equal to that of the seed light. In all of these practical access networks, the power penalty due to beat noises from backreflections and the optimum ONU gain are determined by equations (3.4) and (3.5). Based on the equations, in addition to the TLL, the parameters such as the linewidth, the modulation bandwidth and the receiver bandwidth all have an impact.

3.3 Experimental results

The above discussions allow us to analyze the system impairment due to beat noises between backreflections and the upstream signal in single-fiber bidirectional WDM-PON access networks. We have shown theoretically that the RIN, the power penalty and the

optimum ONU gain that minimizes this penalty is not only determined by the TLL as previously reported in [105], but is also dependent on the linewidth of the seed light, the chirp effect at the ONU as well as the receiver bandwidth. In order to confirm our theoretical analysis, different types of light sources at the OLT and various wavelength-independent ONU configurations are investigated.

3.3.1 Experimental setup

As discussed earlier, in a single-fiber bidirectional WDM-PON system, there are two dominant sources of backreflections which beat with the upstream signal resulting in the system penalty. To investigate the impact of these backreflections, I set up a WDM-PON system, which is shown in Fig. 3.4. The OLT is composed of a light source, an optical receiver, a bit error rate test set (BERT) and two variable optical attenuators (VOAs). The light source is either a DFB-LD, a spectrum-sliced ASE source or a filtered MW-LS. Either a CW or modulated output signal of the light source is used as the seed light proceeds toward the ONU. Attenuator 1 is used to change the seed light power to the ONU while attenuator 2 is for measuring the power penalty after introducing the backreflections. The ONU includes a transmitter, an EDFA, a VOA and a circulator. The transmitter is a FP-LD or a RSOA and is directly modulated by a 2^{23}-1 NRZ pseudorandom bit sequence (PRBS). Since the FP-LD is very polarization sensitive, a polarization controller is inserted between the circulator and the transmitter when the FP-LD is used as the transmitter. The ONU gain is altered by tuning the EDFA and the VOA at the ONU. The rest of the system is the transmission line, which consists of 3 dB

couplers, VOAs, circulators, 1x8 couplers, and optical delay lines (ODLs). The ODLs are composed of eight SMFs with different length.

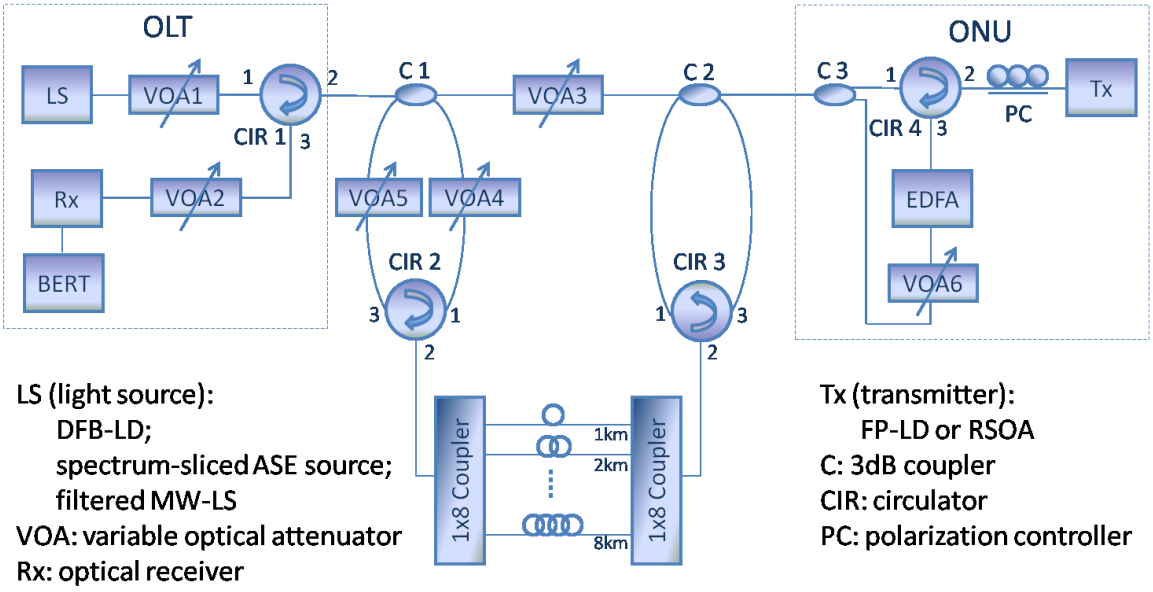

Fig. 3.4 Schematic of the experimental setup

In this experimental setup, both backreflection I and backreflection II are simulated at the same time by only one set of delay fibers (1–8 km), as shown in Fig. 3.4. Since these delay fibers vary in length (i.e., they have different delay times), they could represent the discrete reflection points in the transmission line, which approximately simulates the continuous distributed reflection such as RB. Eight ODLs are found to be sufficient to well represent RB in this setup. The path of backreflection I is as follows: the output light from the OLT goes to port 1 of circulator 2 through the 3 dB coupler 1; then it is delayed by the ODLs and goes back to the OLT after circulator 3, coupler 2 and coupler 1. Backreflection II goes the opposite direction to backreflection I through the ODLs. It starts from 3 dB coupler 2 and then arrives at port 1 of circulator 3. After being delayed,

it goes back to the ONU, and then it is remodulated, reamplified and sent back to the OLT. The transmission line is composed of coupler 1, coupler 2 and attenuator 3. Therefore, the TLL could be changed by attenuator 3. Attenuators 4 and 5 are in charge of adjusting backreflection I and II, respectively. The ORL is defined as the logarithmic ratio of the total returning received power to the incident power at the source. As in a real single-fiber bidirectional PON system, the ORL of the OLT and the ONU are the same, it is important to verify that this condition is satisfied. In the experimental setup, the ORLs are measured at the outputs of the OLT and the ONU, respectively. The ORL of the OLT is measured to be the optical power ratio of the returning signal after the ODLs and the signal output of the OLT. The ORL of the ONU is measured the same way at the output of the ONU. When measuring the ORL at the OLT side, the transmitter of the ONU is not operational. The same condition applies to the measurement of the ORL at the ONU side. The power penalty is measured at the OLT receiver to characterize the impact of the beat noise. Only the beat noise between the backreflections and the upstream signal is investigated, and the degradation of the downstream signal caused by backreflections is not included in this thesis. Because of the eight reflection points used in the experimental setup, the state of polarizations of each backreflection light becomes completely random, which results that the backreflection penalty measured is 3 dB lower compared to the worst case. The BERT is used to monitor the Q factor during the measurement. It should be noted that all power penalty results are measured at Q=6. In addition, a TLL of 7 dB, ORL of -30 dB and receiver bandwidth of 155 MHz are used in the experiment unless stated otherwise. As the system works at low bit rate, the fiber dispersion and intensity noise from the BLS do not have much impact on its performance as discussed in section

2.4, while the penalty from RB is the main factor that plays a role. By operating the system with the backreflection setup enabled or disabled, all the results going to be shown below only reflect the impairment from RB.

3.3.2 Characteristics of system components

In my experimental setup, various seed lights are implemented at the OLT, which is the CW light out of a DFB-LD, a spectrum-sliced ASE source or a filtered MW-LS. In addition, in the WDM-PON system with remodulation scheme, a LiNbO3 modulator is utilized after the light source to modulate the downstream signal. At the ONU, either a RSOA or a FP-LD is used as the modulator for the upstream signal. In this section, I will give a brief overview of the characteristics of these essential components.

The DFB-LD in the experiment is a 4245 tunable laser transmitter from JDS Uniphase Corporation [116]. The evaluation board with DC, Clock and Data inputs can be connected to the computer through the serial cable to be able to control the laser module. This module has 90 ITU channels at 50 GHz spacing, ranging from 1528 nm to 1563 nm. The laser module has an integrated electro-absorption modulator (EAM) and SOA. It also incorporates an integral wavelength locker. The laser module could be operated either as a CW light (w/o applying Clock and Data inputs) or as a transmitter which can be modulated up to 2.5 Gb/s data rate.

For the spectrum-sliced ASE source and the filtered MW-LS, a band pass filter is required to select the wavelength or the optical channel. The VCF100 series voltage-controlled optical filter used is from JDS Uniphase Corporation [117]. This filter is a 100

GHz tunable C-band band pass filter, in which the center wavelength selection is precisely tuned using a stepper motor driven by an external integrated circuit driver. The filter module is compact in size and can easily be mounted on a printed circuit board. The transmission spectrum of the filter is optimized for low insertion loss, high rejection, and low chromatic dispersion. The MW-LS has 16 channels with 50 GHz spacing. As a result, the 100 GHz optical filter is not sufficient to be able to select one channel. An interleaver is used between the MW-LS and the optical filter to act as the first stage filter. The following spectrums in Fig. 3.5 show how one channel is selected from the MW-LS as the seed light. The dashed curve is the free-running spectrum of the MW-LS. The solid one is the spectrum of the MW-LS after the interleaver, where we can see that the interleaver intends to remove half of its channels. After the 100 GHz optical filter, a pretty good single-channel seed light is achieved, shown as the dotted curve.

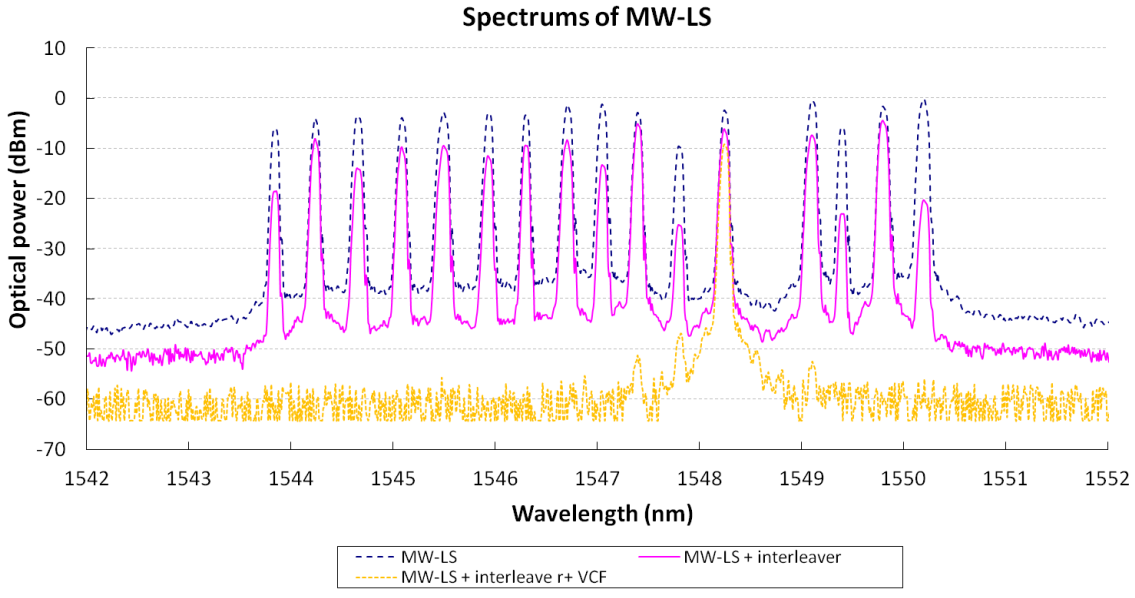

Fig. 3.5 Spectrums of the seed light selection from the MW-LS

Furthermore, in order to have the ability to control the ER of the downstream signal in the WDM-PON with remodulation scheme, a LiNbO3 electro-optic modulator (EOM) is utilized with the DFB-LD to generate the downstream signal instead of direct modulation by its own integrated modulator. The modulator is the 2.5 Gb/s bias-ready modulator from JDS Uniphase Corporation [118]. By applying the bias control circuit, the modulation depth and the bit rate can be changed. The detailed performance of modulated downstream signal from this modulator can be found in section 3.3.4.

The RSOA used in my experiment is from Amphotonix Ltd., which is packaged in the industry standard, low-cost, single mode fiber pigtailed TO-can. It comes with the evaluation board which has access to control the RSOA's current and temperature [119]. The RSOA is offered with a range of gains and output powers and has low polarization-dependent gain as well as low noise figure, which is suitable for use as a directly modulated colorless source in WDM-PON applications at up to 1.25 Gb/s. Fig. 3.6 shows the tested gain characteristics of the RSOA. Fig. 3.6 (a) is the tested gain as a function of the output power at current of 60 mA and 80mA. The RSOA is operated at 60 mA in the experiment, which gives us ~ 12 dB gain out of the RSOA. Fig. 3.6 (b) shows the wavelength-dependent gain by comparing the gain at 1530 nm with that at 1550 nm as a function of the current. We could see that in the current range of 45-80 mA, the difference of gain due to the wavelength is within 0.2 dB. In this experiment, the wavelength of the seed lights for the RSOA is set at 1548.2 nm, the injected power is -15 dBm and the operating current of the RSOA is 60 mA. Under these conditions, the polarization-dependent gain of the RSOA is found to be smaller than 0.1 dB.

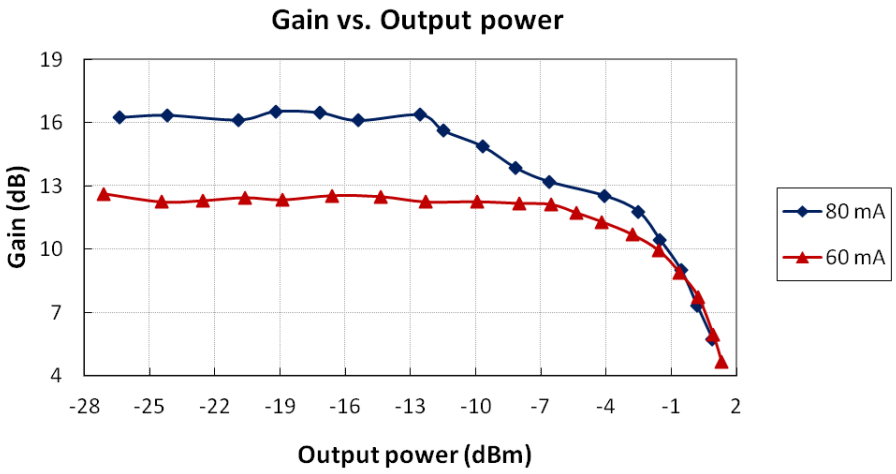

(a)

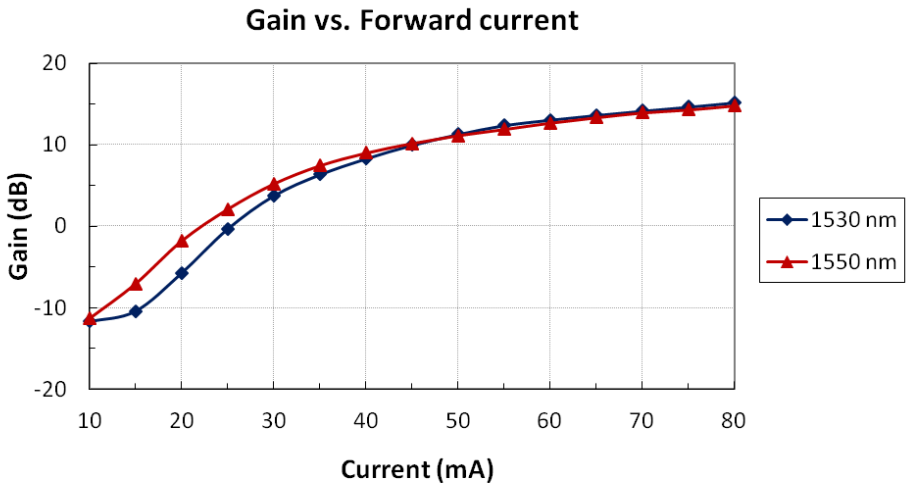

(b)

Fig. 3.6 Gain characteristics of RSOA

As another modulator at the ONU, the FP-LD used in the experiment is packaged in TO-can as well. This product is from Optoway Technology Inc. [120]. As a semiconductor laser, FP-LDs are very sensitive to temperature change. Therefore, the wavelengths would shift under unstable temperature condition. To make sure that the FP-LD is able to

maintain stable injection-locking, temperature control is very important. As a compact and easy-to-use device, FP-LD small form-factor pluggable (SFP) is a normal device in the market. However, due to the lack of ability to control the temperature, it is found to be difficult to use in the experiment. The TO-can packaged FP-LD is soldered on the same evaluation board as the RSOA's, which allows us to precisely control its temperature as well as the driving current. At the same time, we could apply the upstream data to the RF port of the evaluation board to modulate the FP-LD. Moreover, the FP-LD used in the experiment is found to be very sensitive to the polarization state of the injected seed light. A polarization controller is used at the input of the FP-LD to make sure a steadily well locked upstream signal.

3.3.3 Experimental results in WDM-PON with CW seed light

In this section, a single-fiber bidirectional WDM-PON access network with colorless ONUs is implemented. In this network, a CW light from the OLT is injected to the ONU as the seed light, which is modulated and amplified at the ONU and sent back to the OLT as the upstream signal. The modulated downstream signal has a different wavelength from the seed light and is sent to the user side separately. As a result, the upstream signal beats with the backreflections of the CW seed light other than the downstream itself, which allows us to ignore the downstream signal in the following discussion.

As depicted in Fig. 3.4, several candidates have been used in the setup as the seed light at the OLT. In addition, various transmitters are implemented at the ONU. The seed light could be a DFB-LD, a spectrum-sliced ASE source or a filtered MW-LS. Since these

light sources have different linewidths, the different beat noise effects for various WDM-PON schemes could be investigated. The transmitter at the ONU could be a RSOA or a FP-LD, which could demonstrate the different impact on the linewidth change of the seed light at the ONU. The transmitter is directly modulated by a 2^{23}-1 PRBS at a 155 Mb/s bit rate.

3.3.3.1 Impact of backreflections on RSOA-based WDM-PON

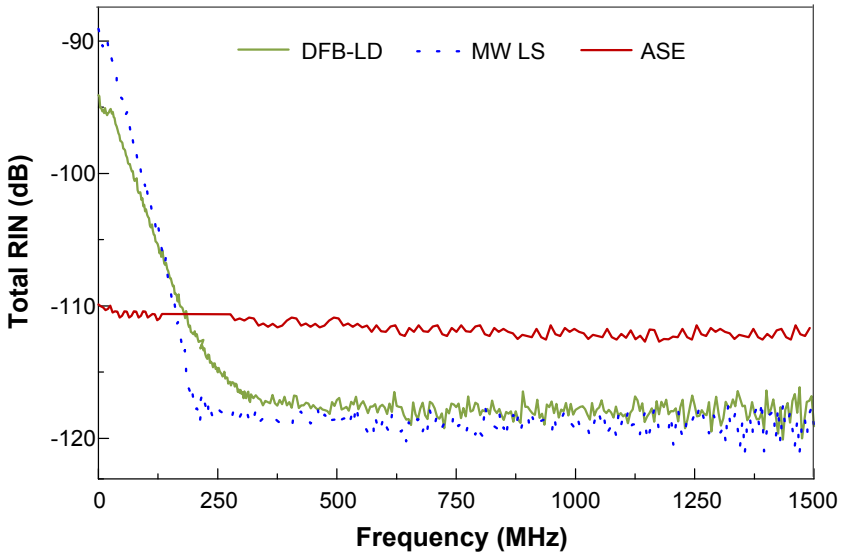

Fig. 3.7 Spectrum of total RIN at mark level for three cases: DFB –LD, ASE and MW-LS injection

In this scheme, a RSOA is used at the ONU as the modulator for the upstream signal. At the OLT, three different light sources are utilized as the seed light, which is a DFB-LD, or a spectrum-sliced ASE source or a filtered MW-LS. The linewidths of these sources are 25 MHz, 60 GHz and 100 Hz, respectively. The linewidths of the upstreams, which include the RSOA chirp effect, are 65 MHz, 60 GHz and 52 MHz, correspondingly. In

the experiment, the linewidths are measured using a HP 8568A spectrum analyzer, an HP 11980A fiber-optic interferometer and a 1.25 GHz bandwidth receiver. The linewidth of the spectrum-sliced ASE source is determined by the optical filter bandwidth.

Figure 3.7 shows the relationship of the total RIN with the frequency at the mark level for these three cases. The total RIN is measured at the OLT receiver. All results are measured at a TLL of 7 dB, an ORL of -30 dB and a net gain of 8 dB. It can be seen that the broader the linewidth of the seed light, the flatter the RIN distribution with frequency and the smaller its value at low frequencies. Hence, when operating the upstream signal at 155 Mb/s, the broader the injection seed light linewidth, the lower the power penalty it gives, under the condition that other system parameters are comparable.

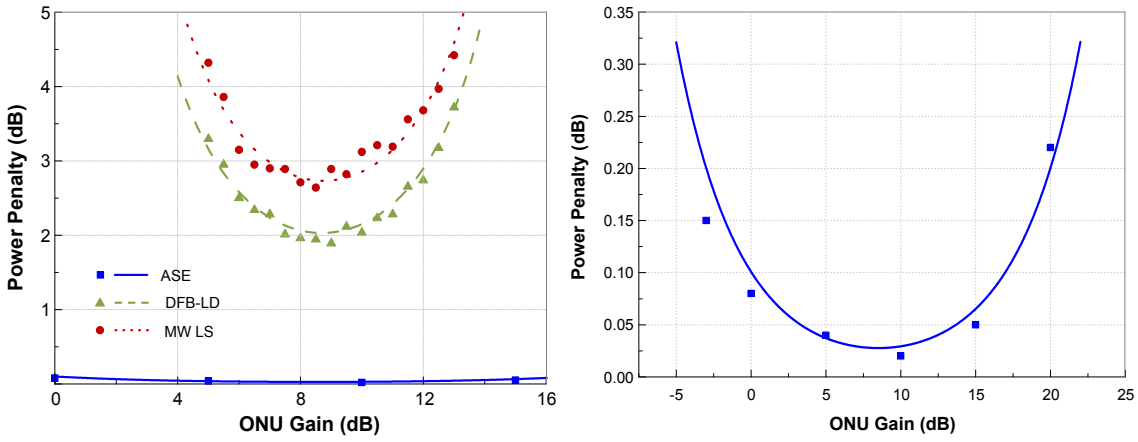

(a) (b)

Fig. 3.8 Power penalty as a function of the ONU gain for different injection sources at OLT (a) all (b) ASE

Figure 3.8 depicts the power penalty as a function of the ONU gain for each case. The scattered symbols are measured results, while the smooth lines are simulation ones as a

comparison (the same elsewhere). In Fig. 3.8 (a), all three cases with identical ONU (RSOA) but different seed lights are displayed. To show the ASE injection case more clearly, it is drawn in Fig. 3.8 (b). It is shown that the optimum ONU gain is 8.5 dB for an ASE-injected RSOA, while it shifts to 8.7 dB and 8.76 dB for the DFB-LD and MW-LS cases, respectively. When the RSOA is injected by the ASE source, the linewidths of the seed light and the upstream signal are almost the same and the optimum ONU gain depends only on the TLL. As for the DFB-LD case, the RSOA chirp effect makes a difference between the linewidths of the seed light and the upstream signal (25-65 MHz), which increases the optimum gain. In the MW-LS injection case, the linewidth of the MW-LS is very narrow compared with the upstream. Hence, the average linewidth of the upstream signal and the seed light is half the upstream one. In this case, the linewidth impact shifts the optimum gain as well. Since the linewidth of the ASE source is quite broad, the power penalty is very small so that I use ORL=-28 dB and a 2.5 GHz receiver bandwidth for the ASE case, while ORL=-30 dB and a 155 MHz bandwidth are used in the other two cases. However, the power penalty from the ASE injection signal is still negligible even though higher ORL and receiver bandwidth are used compared to the other two cases. The minimum power penalty of the DFB-LD and MW-LS cases are ~2 dB and ~2.7 dB, respectively, while that of the ASE case is only ~0.03 dB. The experimental results agree well with our theoretical model. It should be noted that a high ORL value results in a larger power penalty but does not change the position of the optimum ONU gain. The optimum gain depends on the receiver bandwidth based on Eq. (3.5). However, this dependency disappears when the linewidths of the seed light and the upstream signal are the same, which is almost the case for ASE injection. As a result,

even though a higher ORL value and a higher bandwidth receiver are used for ASE injection, the optimum gain for ASE can still be compared to the other two cases.

To verify the effect of the ORL, the variation of power penalty with the ONU gain for various ORLs is plotted in Fig. 3.9. The results are for ORLs of -32, -31 and -30 dB. As expected, a high ORL gives higher penalty, but the optimum ONU gain remains the same. The experimental results are consistent with the simulation ones.

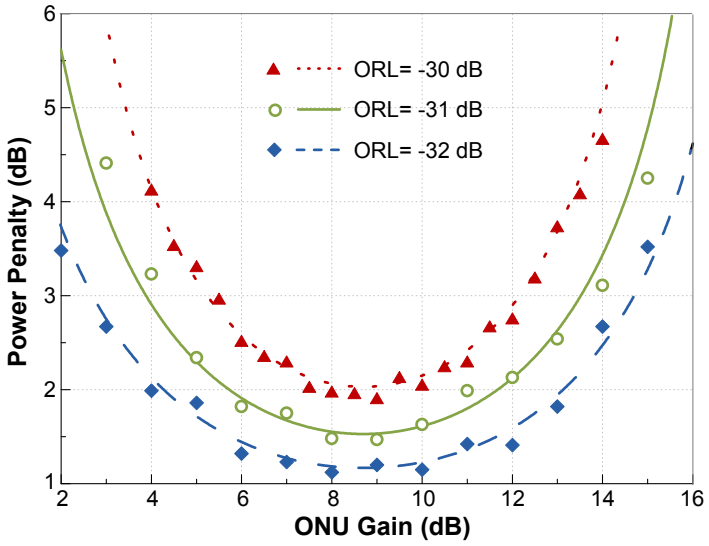

Fig. 3.9 Power penalty versus ONU gain at various ORLs

As previously mentioned, the receiver bandwidth also plays a significant role when the linewidths of the seed light and the upstream signal are different. To investigate the effect of the receiver bandwidth, two different bandwidth receivers, 155 MHz and 2.5 GHz, are used at the OLT. A DFB-LD is used to inject the RSOA of the ONU. Based on the fact that a larger receiver bandwidth collects more noise, we know that a higher bandwidth receiver gives a higher power penalty. Moreover, for specific linewidths of the seed light and the upstream signal, a higher receiver bandwidth leads to a lower optimum ONU gain

as well. The power penalties for different receivers are illustrated in Fig. 3.10. At the optimal ONU gain, the 2.5 GHz receiver results in an increase in the power penalty by ~0.8 dB compared to that of the 155 MHz receiver, and the penalty increases even more at other ONU gains. The optimum ONU gain for the 2.5 GHz receiver case is 8.5 dB, while it is 8.7 dB for the 155 MHz receiver case. As can be seen from the figure, the experimental results agree well with the simulation ones. Hence, for a given WDM-PON configuration, if we use different data rates for the upstream, which requires a different bandwidth receiver at the OLT, the ONU gain needs to be tuned to obtain the minimum power penalty.

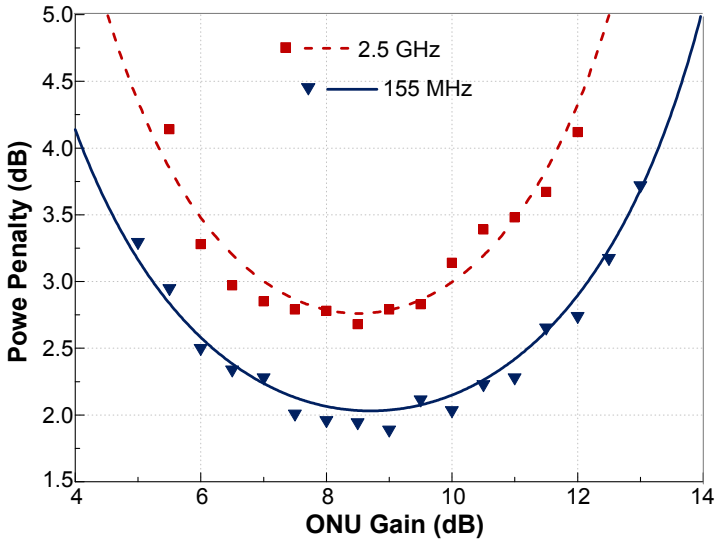

Fig. 3.10 Power penalty as a function of the ONU gain for different receiver bandwidths

In this section, I have shown that in a CW-seeded RSOA-based PON system, when a broad linewidth light is used as the seed light, low power penalty and low optimum ONU gain are achieved. The low power penalty is due to the low RIN of a large linewidth source, while the low optimum ONU gain results from the relatively small chirp effect at

the ONU. Additionally, the effects of the ORL and the receiver bandwidth on the optimum ONU gain are also investigated. Higher bandwidth detectors give higher power penalty as well as lower optimum ONU gain.

3.3.3.2 Impact of backreflections on FP-LD-based WDM-PON

When an injection seed light at the OLT is used to lock the FP-LD at the ONU, a single mode approximation can be used and the dynamic characteristics of an injection-locked FP-LD are described by rate equations that account for the injection power effect on carrier density. The frequency chirp and dynamic behavior of the injection-locked FP-LD strongly depends on the injected power, detuning and the ER [121]. In this section, I use a CW signal from the DFB-LD as the seed light and investigate the impact of different injected powers.

Figure 3.11 shows the optical spectra of the upstream signal. The injection powers are -3 dBm and 0 dBm, respectively. The free-running optical power of the FP-LD is 3 dBm. As the injection ratio is defined as the optical power ratio of the injection one and the free-running one, the injection ratios of -6 dB and -3 dB are achieved, respectively, which ensures a stable injection locking of the FP-LD [122]. The inset is the spectrum comparison of the two peak modes. We can see that when the injected power is higher, the SMSR is higher and the spectrum is narrower. The SMSR is 36.6 dB under the condition that the injected power is -3 dBm, while it is 39.2 dB when the injected power increases to 0 dBm.

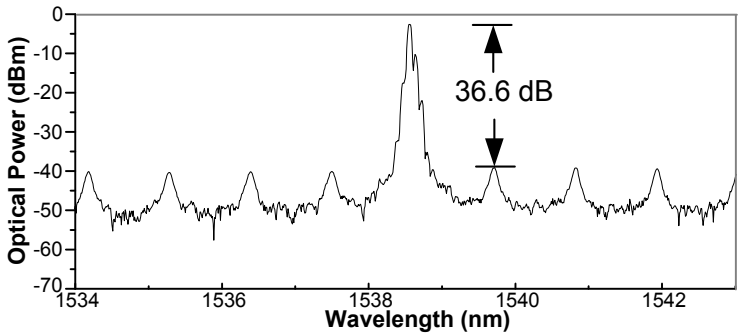

(a)

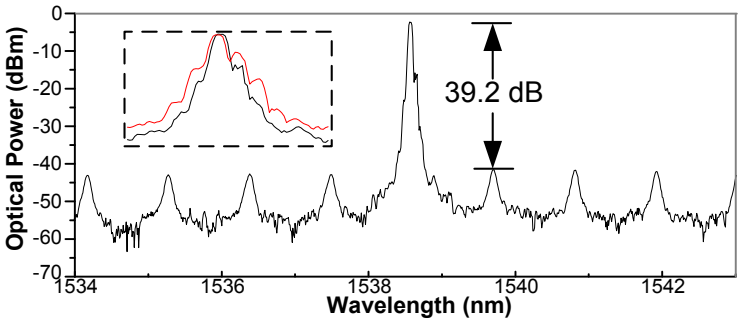

(b)

Fig. 3.11 FP-LD spectrums after injection (a) -3 dBm injected power (b) 0 dBm injected power

Figure 3.12 is the result of power penalty measurement of these two situations. The experimental results match with the ones from our theoretical model. Even though the same linewidth light is injected, both the power penalty and the optimum ONU gain are different because of the difference in the upstream linewidth. This difference can be expected from the shape of the spectrum and the SMSR difference. Under operating conditions, the FP-LD linewidths corresponding to -3 dBm and 0 dBm injection powers are 200 MHz and 111 MHz and the optimum ONU gains are 9.3 and 8.9, respectively. We can see that even if the same DFB-LD is used to injection-lock the FP-LD at the ONU, the optimum ONU gain position is not the same and a ~0.6 dB power penalty

difference at the optimum ONU gain is obtained due to the different injection power. To realize a lower beat noise penalty caused by backreflections, a lower injection power is preferred.

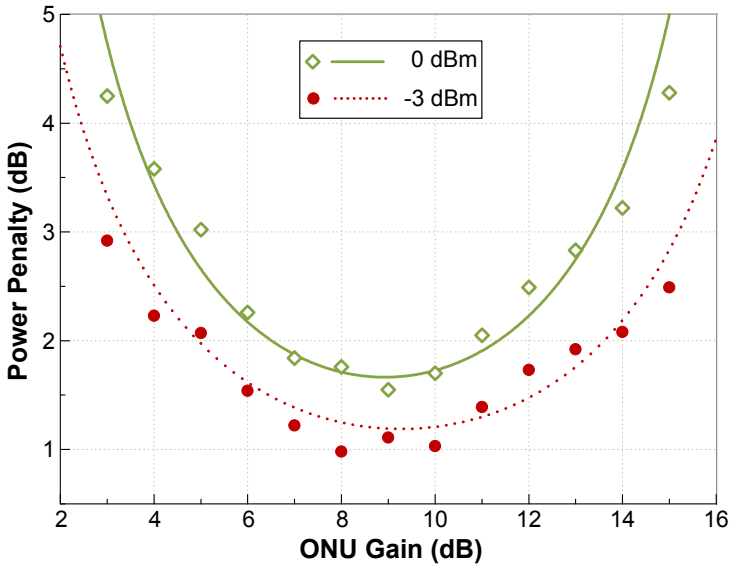

Fig. 3.12 Power penalty versus ONU gain for -3 dBm and 0 dBm injection powers to the FP-LD

3.3.3.3 Comparison of impact of backreflections on RSOA- and FP-LD-based WDM-PON

In the previous discussion, I analyzed the performance of the system when changing the seed light while keeping the ONU side identical. Both RSOA- and FP-LD-based ONUs were investigated. Now I look into the results of using the same seed light but different ONU configurations. The CW output of the DFB-LD is used as the seed light and the results of RSOA and FP-LD are compared in Fig. 3.13. For the FP-LD case, -3 dBm injection power is used. Since the linewidth of the upstream signal for FP-LD is broader than that for RSOA (i.e., 200 MHz versus 65 MHz), a higher optimum ONU gain and

lower power penalty are obtained for the former case. The optimum ONU gain for the RSOA is 8.7 dB and the minimum power penalty is ~2 dB, while for the FP-LD case, the optimum ONU gain is 9.3 dB and the power penalty decreases to ~1.2 dB. Hence, when the ONU is seeded by the same injection signal, broader upstream linewidth gives lower power penalty but higher optimum ONU gain.

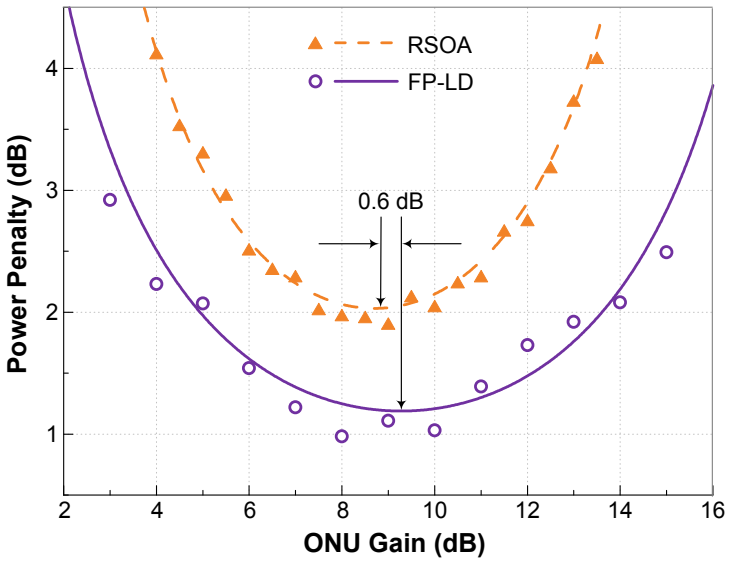

Fig. 3.13 Power penalty as a function of ONU gain for identical OLT and different ONUs

3.3.4 Experimental results in WDM-PON with remodulation scheme

3.3.4.1 Evaluation of WDM-PON's performance with remodulation scheme

As discussed earlier, a more effective way to realize colorless ONUs is to use the downstream signal itself as the seed light. In such scheme, the optical signal modulated with downstream data is reused to carry the upstream data. Recently, several remodulation architectures have been proposed [19-23], [59-63]. In all of these configurations, using NRZ coding for both downstream and upstream data is the simplest

technique because there is no need to setup the more complicated components for other modulation formats. A few publications have demonstrated that by operating the RSOA in its gain-saturation region, the downstream data included in the upstream data can be suppressed through the amplitude squeezing effect [20-23]. The most important thing to consider in such schemes is that whether or not the downstream data can be sufficiently suppressed at the ONU since the unremoved downstream data is part of the intensity noise for the detected upstream signal. I utilize this technology to investigate the backreflection impact in WDM-PON access network with remodulation scheme. In the experiment, the downstream signal is generated by externally modulating the DFB-LD through an EOM at the OLT. The downstream signal, which is also served as the seed light, is then remodulated at the ONU to generate the upstream signal.

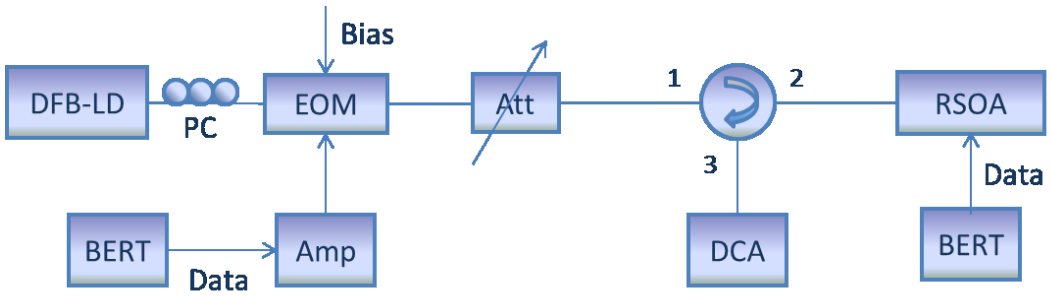

Fig. 3.14 Simplified WDM-PON with remodulation scheme

To evaluate the performance of my system using remodulation technology, I setup a simplified system which does not include the backreflection setup as shown in Fig. 3.14. The DFB-LD is connected to a polarization controller to adjust the light's axis to align with the EOM. The attenuator is to change the injected power to the RSOA. The single BERT is used to apply downstream and upstream data at the same time, i.e., the two data

outputs (data output and its complementary output) of the BERT are supplied to the EOM and the RSOA, respectively. The data for the downstream is added to the EOM through a modulator driver, which is an electrical amplifier. A 2 volts peak-to-peak data is added directly to the RSOA to generate the upstream signal. The bit rate of the downstream signal and that of the upstream signal are both 622 Mb/s with complementary data inputs, respectively. The RSOA is operated at current of 60 mA. After the remodulation process, the upstream signal is observed at port 3 of the circulator by a digital communication analyzer (DCA).

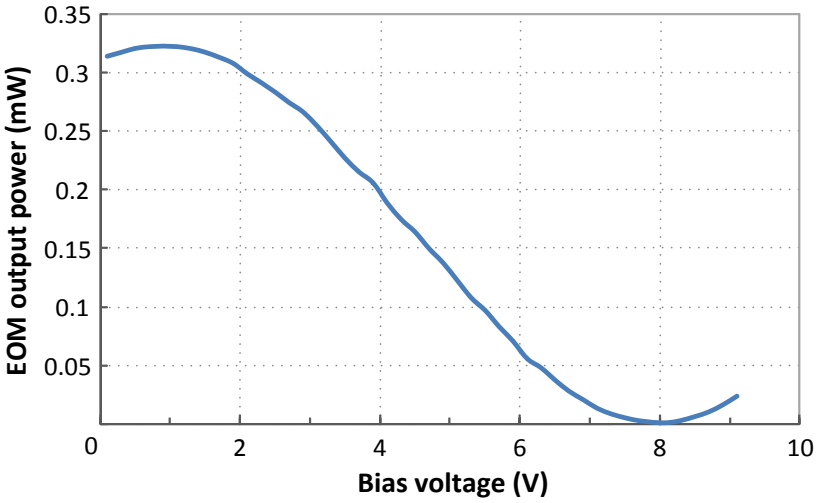

Fig. 3.15 EOM response test curve

The EOM used in the experiment is a 2.5 Gb/s bias-ready optical modulator. The tested response curve of the EOM is shown in Fig. 3.15. The two peaks in the curve are at 0.9 V and 8.1 V, respectively. According to the curve, if we want the modulated eye as open as possible, the optimum operation range of the EOM is around 4.5 V.

The gain characteristics of the RSOA are tested and demonstrated in Fig. 3.16. The curve is tested under the condition that the wavelength of the seed light is 1550 nm and the operating current of RSOA is 60 mA. From the figure, we can see that the small signal gain of the RSOA is around 12.5 dB. If the saturation gain is defined as when the gain decreases to 3 dB less than that of the small signal gain, then the saturation input power of the RSOA is around -10 dBm. In the gain-saturation region, as the injection power into RSOA increases, the optical gain of RSOA decreases. As the injection power at "0" level of downstream is lower than that at "1" level, the gain difference between "0" and "1" levels results in suppression of the ER.

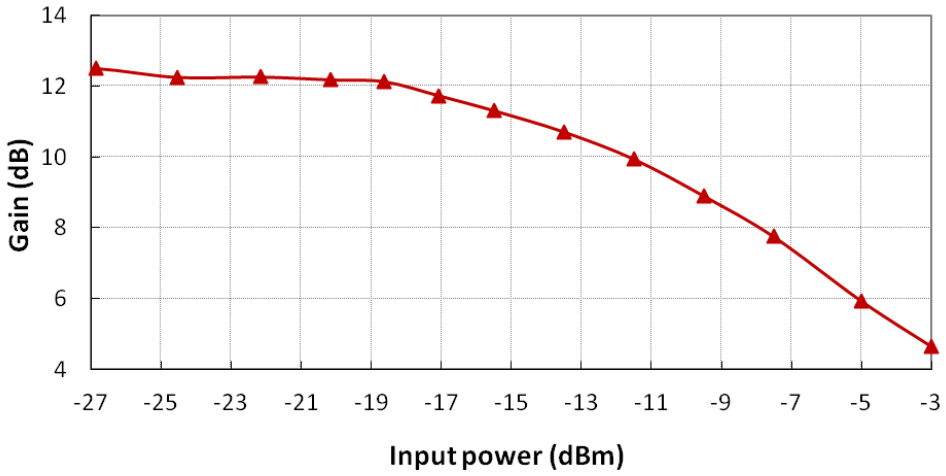

Fig. 3.16 RSOA gain versus input optical power

In the experiment, bias voltage and data of the EOM are tuned to change the ER of the downstream signal. The quality of the upstream signal is then observed on the DCA. For example, when the ERs of the downstream signals are 2.2 dB, 3.1 dB, and 5.0 dB, the eye diagrams of the upstream signals are shown in Fig. 3.17. We can see that when

downstream ER=5.0 dB, there are clearly two sets of eyes in the upstream signal. That is because the downstream data could not be suppressed well so that one set of eye is modulated on the "1" level of the downstream data while the other set of eye is modulated on the "0" level of the downstream data. In this case, the upstream is too "noisy" to be considered for a good upstream signal. From the eye diagrams, we can see there are abnormal "wing" shape noises on both "1" level and "0" level. As the downstream ER increases, that noise becomes bigger. This is due to the response at the reflected facet of the RSOA. Since the same BERT is supplying data to both downstream and upstream modulators, when detecting the upstream signal at the DCA, not only is the upstream signal synchronized, the downstream signal is also synchronized which appears to be that noise.

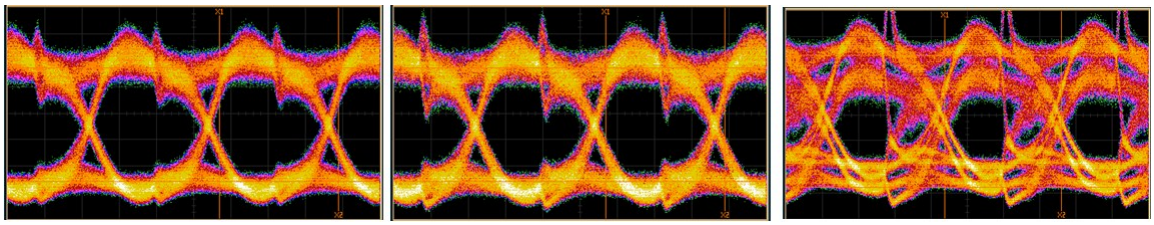

(a) ER=2.2 dB (b) ER=3.1 dB (c) ER=5.0 dB

Fig. 3.17 Eye diagrams of upstream signal with various downstream ER

To overcome this disadvantage, I setup a similar system by supplying the upstream data with a pattern generator other than the BERT. The BERT is only used for the downstream data. In this case, the downstream and upstream signals are with different clock information and they could be operated with different bit rate as well. The RSOA is still modulated at 622 Mb/s as the upstream signal. The downstream EOM is modulated at 1.25 Gb/s, 622 Mb/s and 155 Mb/s, respectively. The ER of the downstream data is 2.65

dB. The eye diagrams of the upstream signal are shown in Fig. 3.18. The figure demonstrates that the lower the downstream signal bit rate, the less noise reflected on the upstream signal.

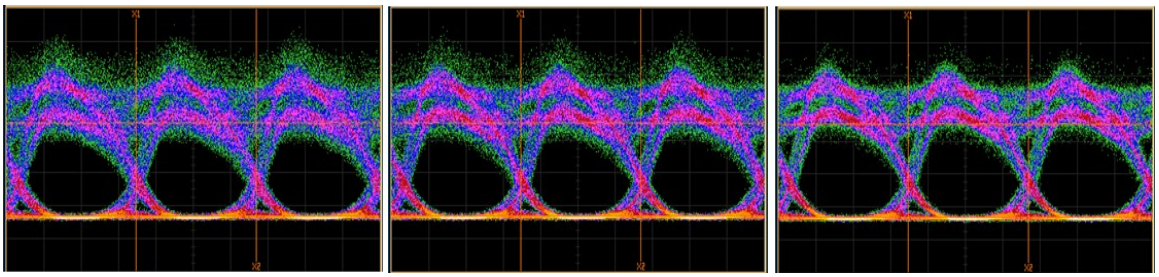

(a) bit rate=1.25 Gb/s (b) bit rate=622 Mb/s (c) bit rate=155 Mb/s

Fig. 3.18 Eye diagrams of upstream signal with different downstream signal bit rate

Then I setup the backreflection test bed as shown in Fig. 3.4 with the remodulation scheme. The ER of the downstream signal is set to 2.2 dB to suppress the residual downstream data components so that the remodulation noise induced to the upstream signal is mitigated [123]. Such low ER could reduce the downstream signal quality and limit the power budget. However, to compare with the previous results, in which the on–off keying (OOK) modulation is used for the upstream signal, the same modulation method is selected for the downstream signal in the remodulation scheme. As a result, this low ER is a straightforward approach to realize the remodulation scheme and to be able to evaluate the impact of the backreflections on the upstream signal. Under operation conditions, the linewidth of the downstream signal is 35 MHz. At the ONU, the downstream signal is remodulated through the data added on the RSOA or the FP-LD.

3.3.4.2 Impact of backreflections on RSOA-based WDM-PON with remodulation scheme

Figure 3.19 includes both the experimental and simulation results for the RSOA-based WDM-PON setup. It can be seen that the experimental results agree well with the simulations ones. The linewidth of the remodulated RSOA upstream is 80 MHz. The results for TLLs of 7 dB and 9 dB are compared. A 2 dB difference of the optimum ONU gain is observable in the figure. In addition, the smallest power penalty of the 9 dB TLL case is ~1.6 dB higher than that of the 7 dB TLL case. Away from the optimum ONU gain point, the sharper slopes result in a faster increase of the power penalty compared to the 7 dB TLL case.

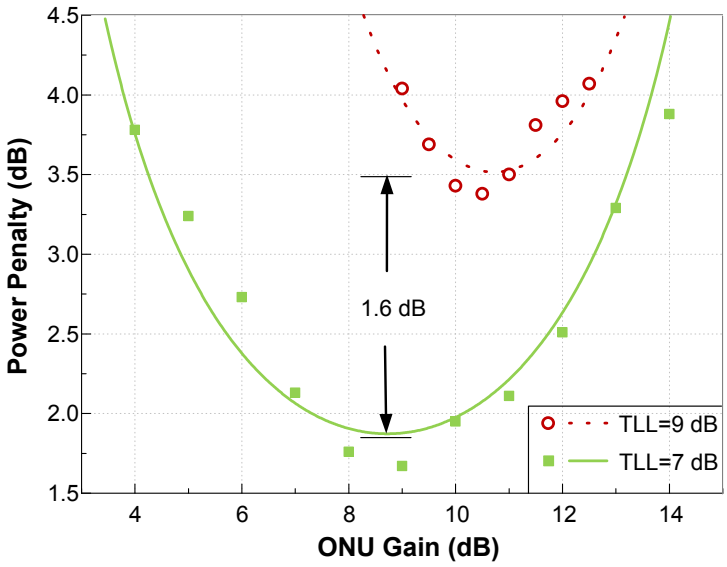

Fig. 3.19 Power penalty as a function of ONU gain for different TLLs

3.3.4.3 Impact of backreflections on FP-LD-based WDM-PON with remodulation scheme

The same downstream signal from the DFB-LD is injected into the ONU to lock the FP-LD. Similar to the CW injection case, I compare the results from different injected powers in Fig. 3.20. The same injected power of 0 dBm and -3 dBm are used in the experiment. Since the seed light is a modulated one, which has a broader linewidth, a lower SMSR and broader upstream linewidth are obtained compared to the CW case under the condition that the injection power is the same. The SMSR becomes 38.5 dB when the injection power is 0 dBm, while that of the 3 dB lower injection power case becomes 34.9 dB. The upstream linewidths are measured to be 130 MHz and 248 MHz, respectively. With a higher injection power, I obtain ~0.5 dB power penalty difference as well as a 0.4 dB lower optimum ONU gain. The experimental results agree well with the simulation ones.

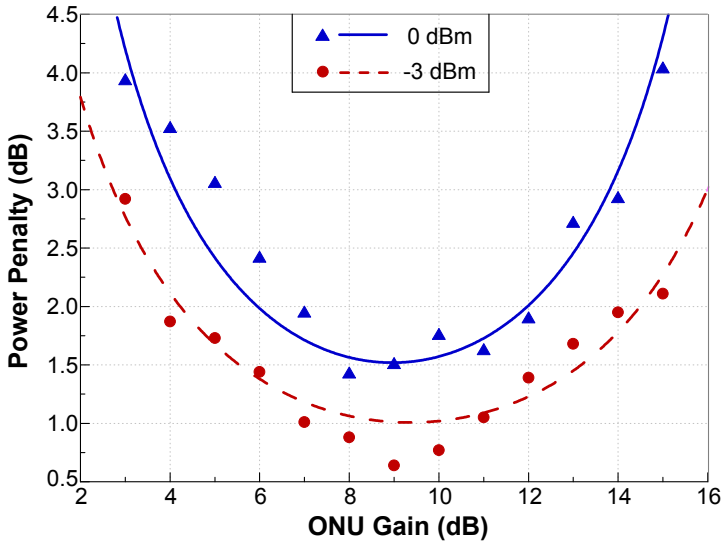

Fig. 3.20 Power penalty versus ONU gain for -3 dBm and 0 dBm injection powers to the FP-LD

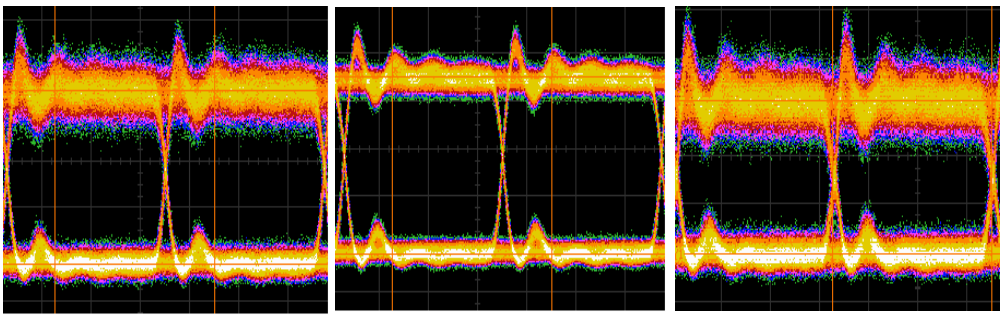

Fig. 3.21 Measured eye diagrams at different ONU gains (a) G=5 dB (b) G=9 dB (c) G=14 dB

As an example, when a -3 dBm power of the modulated DFB-LD signal is injected into the ONU to lock the FP-LD, several measured eye diagrams with regard to different ONU gains 5, 9 and 14 are shown in Fig. 3.21. The quality of the eyes can be distinguished very easily. The ONU gain of 9 dB achieves the best performance based on these three eye diagrams.

3.3.4.4 Comparison of impact of backreflections on WDM-PON with CW seed light and remodulation scheme

Using the same 1.25 Gb/s downstream signal out of the DFB-LD, the beat noise impairments of both RSOA- and FP-LD-based ONUs are investigated. The results are shown in Fig. 3.22. The optimum ONU gains are ~8.7 dB and ~9.4 dB for the system with a RSOA and a FP-LD, respectively. The smallest power penalty of the FP-LD setup is ~0.9 dB lower than that of the RSOA one. In this comparison, a -3 dBm power is injected into the FP-LD and the SMSR is 34.9 dB.

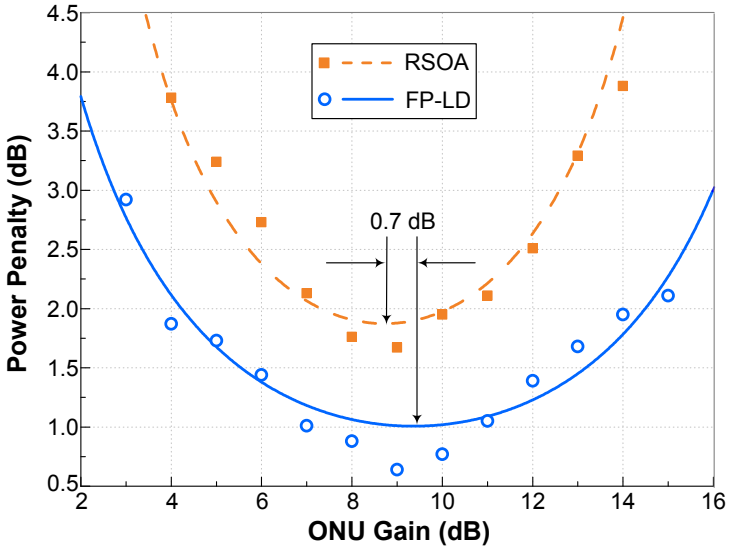

Fig. 3.22 Power penalty as a function of ONU gain for identical OLT and different ONUs

Table 3.1 Linewidth measurement results

OLT		ONU	
CW DFB-LD	25 MHz	RSOA	65 MHz
		FP-LD	111 MHz
Modulated DFB-LD	35 MHz	RSOA	80 MHz
		FP-LD	130 MHz

Now I compare the results of CW and downstream signal injection for both the RSOA and FP-LD at the ONU. The injection power to the FP-LD is 0 dBm. In both parts of Fig. 3.23, TLL=9 dB, ORL=-30 dB and the receiver bandwidth is 155 MHz. The linewidths under all four different conditions are shown in Table 3.1. It can be seen that when the downstream signal is injected into the ONU, lower beat noise penalty is achieved because of the broader linewidth of downstream as well as that of the upstream. This lower penalty is more obvious in the RSOA case because the seeded RSOA linewidth is

narrower than that of the FP-LD. The experimental results in both figures agree very well with the simulations ones. Hence, from the backreflection penalty point of view, the systems use DFB-LD as the seed light with the remodulation technique have more tolerance compared to the usual CW injection ones.

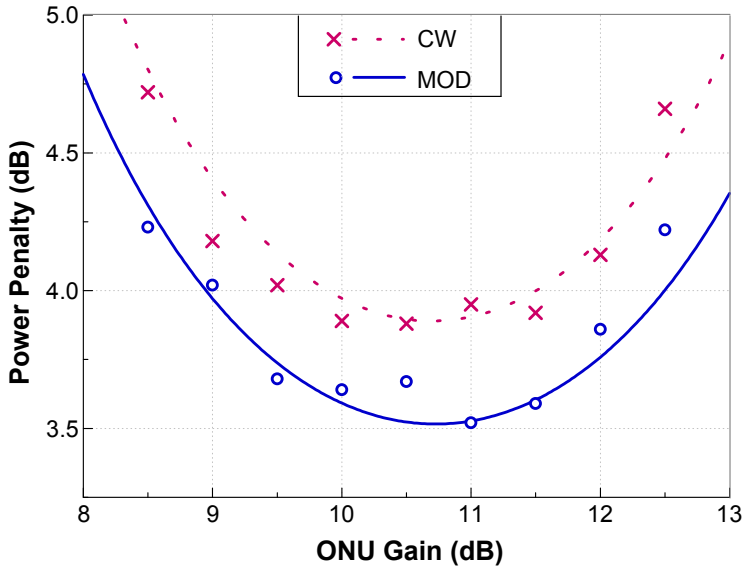

(a) RSOA

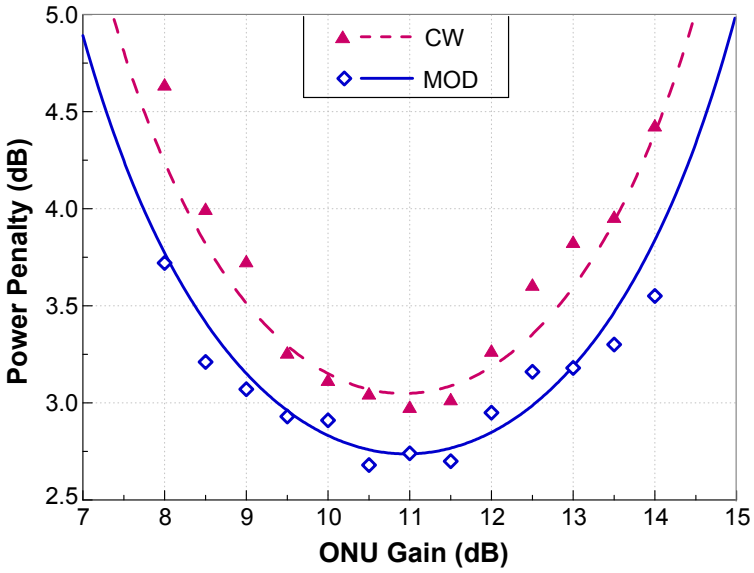

(b) FP-LD

Fig. 3.23 Power penalty comparison between CW and modulated signal injection

3.4 Summary and discussion

In conclusion, I have measured the RIN, the power penalty due to the beat noises between backreflections I and II and the upstream signal in a single-fiber bidirectional WDM-PON, using various light sources at the OLT to remodulate or lock the wavelength-independent devices, such as a RSOA or a FP-LD, at the ONU. The dependence of the power penalty on the source linewidths, receiver bandwidth, ONU gain and ORL have been investigated experimentally. In addition, I have measured the optimum gain at the ONU, which results in the minimum power penalty. The backreflection penalty decreases as the linewidth of the seed light broadens. When the linewidths of the upstream signal and the seed light are the same (such as ASE injection), the optimum ONU gain depends only on the TLL. However, the required optimum ONU gain and minimum penalty are also dependent on the linewidths of the seed light and the upstream signal because they are usually different in practical cases. As the linewidth broadens by the chirp effect, the backreflection penalty decreases, but the optimum ONU gain increases. It has been also shown that the downstream ER results in broadening of the linewidth, which in turn decreases the penalty and increases the optimum ONU gain. This makes the PON systems with remodulation configurations have more tolerance to backreflections when DFB-LD is used as the seed light. The impact of the receiver bandwidth is also explored. As the receiver bandwidth increases, not only does the power penalty increase due to the increase in received noise, but also the optimum ONU gain shifts to the lower side. As a result, the impact of the beat noises can be reduced by broadening the linewidth of the seed light, to spread out the beat noise power over a

frequency range wider than the receiver bandwidth. Therefore, it is advantageous to use sources with broader linewidth relative to the receiver bandwidth given that other system performance is not compromised. In injection locking of FP-LD studies, I show that the system performance does have a difference due to the different injection power that is applied. This analysis makes us realize that the operation condition is also important even if the system components are all fixed.

In all of the experiments, the gain of the amplifier at the ONU is chosen to be able to reach the highest ONU gain test point. Then the ONU gain is varied by tuning the attenuator to achieve the whole ONU gain test range. This ensures that the ONU ER, the chirp and hence the linewidth remains constant for different ONU gains. In contrast, if the driving conditions of the ONU are changed, the impact of backreflections could be different at a specific ONU gain. For example, if the ONU gain is increased by increasing the driving current of the RSOA or the FP-LD, the chirp increases and the effective linewidth broadens, which leads to a reduction in power penalty and a shift of the optimum ONU.

In addition, the beat noise caused by backreflections highly depends on the polarization states of the upstream signal and that of the backreflections. The light sources used in the experiments could have different polarization states. However, as discussed earlier, the use of optical delay fibers with various length results in complete random polarization states for each backreflection light. Therefore, all of the backreflection penalties measured in this experiment are 3 dB lower than those of the worst case. In contrast, if all

backreflections have the same polarization states as the upstream signal, it will be the worst case and it will result in maximum beat noise.

Hence, I experimentally demonstrate that the linewidths of the seed light and the upstream signal have impact on the penalty as well as the optimum ONU gain. These results are in agreement with our theoretical modeling and are valid for all the colorless ONU architectures.

CHAPTER 4 CONCLUSIONS

4.1 Thesis summary

In this thesis, the main objective was to analyze the system impairment due to the intensity noises generated from the beating between backreflections and the signal in single-fiber bidirectional WDM-PON access networks. The objective has been achieved by a comprehensive investigation and analysis of the system penalty caused by backreflections in a WDM-PON system with various colorless architectures. The main body of this thesis was divided into two chapters: Chapter 2 gave a background and overview of WDM-PONs while Chapter 3 focused on my experimental work.

Chapter 2 provided an introduction to WDM-PON technologies. It was pointed out that due to the increasing demand for higher bandwidth, access network is evolving from traditional copper wire to PON-based FTTH. While TDM-PON is the most popular PON architecture, WDM-PON is believed by many to be the solution for higher bandwidth. The architectures of TDM-PON and WDM-PON were described and contrasted. It was pointed out that while WDM-PON has many technical advantages, the cost issue in WDM-PONs remains a significant barrier to wider adoption and deployment. Recent technologies developed to realize colorless architectures, in WDM-PONs, were discussed. The most popular and cost-effective colorless configurations in WDM-PONs, such as injection-locking of FP-LDs, wavelength-seeding of RSOAs and wavelength-reused remodulation schemes, were reviewed and compared. Finally, the various impairments in single-fiber bidirectional WDM-PONs, including the fiber loss, dispersion, the intensity noise from BLS and

colorless ONUs and RB, were discussed. Among them, it was stated that RB is inevitable in the fiber so that it's very important to be considered and analyzed.

In Chapter 3, my experimental work on the investigation of system impairment due to backreflections in single-fiber bidirectional WDM-PON access networks was presented. It started with a literature review of recent work on the impact of backreflections in single-fiber loopback access networks, where the studies on the penalties caused by backreflections specifically in WDM-PONs were detailed. It was pointed out that these studies had limitation which is only valid in a specific scheme. Moreover, there was no study on Rayleigh backreflections in WDM-PONs with remodulation scheme. Afterwards, the definitions of the two types of backreflections considered in my study were introduced, i.e., backreflection I and II, followed by the principles of their relationship with the ONU gain. The theoretical analysis of backreflection penalty which was developed by another group member was also included. Then the WDM-PON system, which represented various colorless configurations, such as injection-locking of FP-LD, wavelength-seeding of RSOA and OOK remodulation scheme, was depicted. My backreflection setup was discussed and the characteristics of major components in the experimental setup were outlined, including the different seed lights at the CO (DFB-LD, spectrum-sliced ASE, and filtered MW-LS), the EAM, as well as the modulators at the ONU (RSOA and FP-LD). Finally, the experimental results for evaluation of backreflection penalty in single-fiber bidirectional WDM-PONs were demonstrated and discussed. The RIN, the power penalty and the optimum ONU gain were investigated. It was found that these parameters are dependent on the transmission line loss (TLL), the linewidth of the seed light, the chirp effect at the ONU

and the bandwidth of the detector. Various colorless configurations were studied to explore those dependencies. The results in different colorless architectures were compared as well.

In conclusion, in this research, it was found that the WDM-PON using spectrum-sliced ASE as the seed light is much more tolerant to backreflections compared to other configurations. This advantage is due to the broader linewidth of the ASE source. Therefore, from the backreflection penalty point of view, injection-locking of FP-LD by spectrum-sliced ASE is the best choice for the WDM-PON configuration. However, due to the non-coherent characteristic of the ASE source, it is limited to the bit rate. Normally, for a WDM-PON works at 2.5 Gb/s or higher, DFB-LDs have to be implemented instead of ASE sources. Hence, different WDM-PON configurations need to be properly chosen in order to realize the required system performance.

4.2 Future work

My research focused on the investigation of system impairment due to backreflections in single-fiber bidirectional WDM-PON access networks. However, a number of issues remain unexplored and can be topics for future investigations:

- In my work, the remodulation scheme was the traditional one which utilized NRZ intensity modulation for both downstream and upstream signals. As discussed in Chapter 2, bringing different modulation formats, such as DPSK, IRZ, etc., have shown the ability to facilitate the erasure of downstream pattern. The studies on the impact of backreflections in such WDM-PONs with different remodulation schemes could be analyzed and compared as well. Especially, the comparison of

intensity modulation and phase modulation could be interesting and further complete the investigation of backreflection penalty in remodulation configurations.

- The current theoretical model developed in our group is valid for intensity modulation. There is a need to derive a general formulation that includes other modulation formats such as different phase modulation formats as well. The model should take into account all the parameters such as the source linewidth, the chirp, receiver bandwidth as well as the ER.

BIBLIOGRPHY

[1]. A. Banerjee, Y. Park, F. Clarke, H. Song, S. Yang, G. Kramer, K. Kim, and B. Mukherjee, " "Wavelength-division-multiplexed passive optical network (WDM-PON) technologies for broadband access: a review," *J. Opt. Netw.*, vol. 4, no. 11, pp. 737–758, Nov. 2005.

[2]. S.-J. Park, C.-H. Lee, K.-T. Jeong, H.-J. Park, J.-G. Ahn, and K.-H. Song, "Fiber-to-the-home services based on wavelength-division-multiplexing passive optical network," *IEEE J. Lightwave Technol.*, vol. 22, no. 11, pp. 2582-2591, Nov. 2004.

[3]. C. Lee, W. V. Sorin, and B. Y. Kim, "Fiber to the home using a PON infrastructure," *IEEE J. Lightwave Technol.*, vol. 24, no. 12, pp. 4568-4583, Dec. 2006.

[4]. C.-H. Lee, S.-M. Lee, K.-M. Choi, J.-H. Moon, S.-G. Mun, K.-T. Jeong, J. H. Kim, and B.Kim, "WDM-PON experiences in Korea," *J. Opt. Netw.*, vol. 6, no. 5, pp. 451–464, 2007.

[5]. T. Koonen, "Fiber to the home/fiber to the premise: what, where, and when?," in. *Proc. IEEE*, vol. 94, no. 5, pp. 911–934, May 2006.

[6]. G. Chang, A. Chowdhury, Z. Jia, H. Chien, M. Huang, J. Yu, and G. Ellinas, "Key technologies of WDM-PON for future converged optical broadband access networks," *J. Opt. Commun. Netw.*, vol. 1, no. 4, pp. c35–c50, Sep. 2009.

[7]. J. Kani, M. Teshima, K. Akimoto, M. Ishii, N. Takachio, and K. Iwatsuki, "Super-dense WDM access network for wide-area gigabit access services," in *Proc. ISSLS* '2002, Session 9-2, 2002.

[8]. H. Nakamura, H. Suzuki, J. Kani, and K. Iwatsuki, "A wide-area carrier-distributed WDM-based access network accommodating GbE and 10 GbE services," in *Proc. OFC/NFOEC*, paper OFA4, 2005.

[9]. L. Y. Chan, C.K. Chan, D.T.K. Tong, F. Tong, L.K. Chen, "Upstream traffic transmitter using injection-locked Fabry–Pérot laser diode as modulator for WDM access networks," *IEE Electron. Lett.,* vol. 38, no. 1, pp. 43-45, Jan. 2002.

[10]. E. Wong, X. Zhao, C. J. Chang-Hasnain, W. Hofmann, and M. C. Amann, "Optically injection-locked 1.55- μm VCSELs as upstream transmitters in WDM-PONs," *IEEE Photon. Technol. Lett*., vol. 18, no. 22, pp. 2371–2373, Nov. 2006.

[11]. H. D. Kim, S. G. Kang, and C. H. Le, "A low-cost WDM source with an ASE injected Fabry–Pérot semiconductor laser," *IEEE Photon. Technol. Lett*., vol. 12, no. 8, pp. 1067–1069, Aug. 2000.

[12]. D. J. Shin, Y. C. Keh, J. W. Kwon, E. H. Lee, J. K. Lee, M. K. Park, J.W. Park, K. Y. Oh, S.W. Kim, I. K. Yun, H. C. Shin, D. Heo, J. S. Lee, H. S. Shin, H. S. Kim, S. B. Park, D. K. Jung, S. Hwang, Y. J. Oh, D. H. Jang, and C. S. Shim, "Low-cost WDM-PON with colorless bidirectional transceivers," *IEEE J. Lightwave. Technol.*, vol. 24, no. 1, pp. 158–165, Jan. 2006.

[13]. Z. Xu, Y. J. Wen, C. Chae, Y. Wang, and C. Lu, "10 Gb/s WDMPON upstream transmission using injection-locked Fabry–Pérot laser diodes," in *Proc. OFC/NFOEC*, paper JThB72, 2006.

[14]. P. Healey, P. Townsend, C. Ford, L. Johnston, P. Townley, I. Lealman, L. Rivers, S. Perrin, and R. Moore, "Spectral slicing WDM-PON using wavelength-seeded reflective SOAs," *IEE Electron. Lett.*, vol. 37, no. 19, pp. 1181–1182, Sep. 2001.

[15]. J. Prat, C. Arellano, V. Polo, and C. Bock, "Optical network unit based on a bidirectional reflective semiconductor optical amplifier for fiber-to-the-home networks," *IEEE Photon. Technol. Lett*., vol. 17, no. 1, pp. 250–252, Jan. 2005.

[16]. F. Payoux, P. Chanclou, M. Moignard, and R. Brenot, "Gigabit optical access using WDM PON based on spectrum slicing and reflective SOA," in *Proc. ECOC*, vol. 3, paper We 3.3.5, pp. 455–456, Sep. 2005.

[17]. H. S. Shin, D. K. Jung, D. H. Shin, S. B. Park, J. S. Lee, I. K. Yun, S. W. Kim, Y. J. Oh, and C. S. Shin, "16×1.25 Gbit/s WDM-PON based on ASE-injected R-SOAs in 60 C temperature range," in *Proc. OFC/NFOEC*, paper OTuC5, 2006.

[18]. K. Y. Cho, Y. Takushima, and Y. C. Chung, "Enhanced operating range of WDM PON implemented by using uncooled RSOAs," *IEEE Photon. Technol. Lett*., vol. 20, no. 18, pp. 1536–1538, Sep. 2008.

[19]. W. Hung, C. K. Chan, L. K. Chen, and F. Tong, "An optical network unit for WDM access networks with downstream DPSK and upstream remodulated OOK data using injection-locked FP laser," *IEEE Photon. Technol. Lett.*, vol. 15, no. 10, pp. 1476–1478, Oct. 2003.

[20]. J. J. Koponen and M. J. Soderlund, "A duplex WDM passive optical network with 1:16 power split using reflective SOA remodulator at ONU," in *Proc. OFC/NFOEC*, paper MF99, 2004.

[21]. W. Lee, M. Y. Park, S. H. Cho, J. Lee, C. Kim, G. Jeong, and B.W. Kim, "Bidirectional WDM-PON based on gain-saturated reflective semiconductor optical amplifiers," *IEEE Photon. Technol. Lett.*, vol. 17, no. 11, pp. 1476–1478, Nov. 2005.

[22]. T. Y. Kim and S. K. Han, "Reflective SOA-based bidirectional WDM-PON sharing optical source for up/downlink data and broadcasting transmission," *IEEE Photon. Technol. Lett.*, vol. 18, no. 22, pp. 2350-2352, Nov. 2006.

[23]. J. H. Yu, N. Kim, and B. W. Kim, "Remodulation schemes with reflective SOA for colorless DWDM PON," *J. Opt. Netw.*, vol. 6, no. 8, pp. 1041–1054, Aug. 2007.

[24]. S. Radic, N. Vukovic, S. Chandrasekhar, A. Velingker, and A. Srivastava, "Forward error correction performance in the presence of Rayleigh-dominated transmission noise," *IEEE Photon. Technol. Lett.*, vol. 15, no. 2, pp. 326–328, Feb. 2003.

[25]. "Cisco visual networking index: Forecast and methodology, 2011-2016," Cisco white papers, May 2012 [Online]. Available: http://www.cisco.com/en/US/solutions/collateral/ns341/ns525/ns537/ns705/ns827/white_paper_c11-481360.pdf

[26]. Infonetics Research (Staff of Broadband Access research division), PON, FTTH, and DSL Aggregation Equipment and Subscribers Campbell, CA, Nov. 2011 [Online]. Available: http://www.infonetics.com/research.asp?cvg=Broadband

[27]. C. F. Lam, "Passive optical networks: principles and practice," *USA: Academic Press,* an imprint of Elsevier. 324 p. ISBN: 978-0-12-373853-0, (ed.) 2007.

[28]. K. Okamoto, "Fundamentals of Optical Waveguides," *New York: Academic*, 2006.

[29]. C. Engineer, "Fiber in the loop: An evolution in service and systems," in *Proc. SPIE Fiber Opt. Subscriber Loop*, vol. 1363, pp. 19–29, 1990.

[30]. G. Van der Plas et al., "Demonstration of ATM-based passive optical network in the FTTH trial on the Bermuda," in *Proc. GLOBECOM*, vol. 99, pp. 988–992, 1995.

[31]. ITU-T, "Broadband optical access systems based on passive optical networks," *Recommendation G. 983.1*, 1998.

[32]. IEEE, "Physical medium dependent (PMD) sublayer and medium, type 1000 BASE-PX10 and 1000 BASE-PX20 (long wavelength passive optical network)," *IEEE Recommendation 802.3 ah*, 2002.

[33]. ITU-T, "Broadband optical access systems based on passive optical networks," *Recommendation G. 984.2*, 2003.

[34]. ITU-T, "10-Gigabit-Capable Passive Optical Networks (XG-PON)," *Recommendation G.987 series*, 2010.

[35]. F. J. Effenberger, "The XG-PON system: Cost effective 10 Gb/s access," *IEEE J. Lightwave. Technol.*, vol. 29, no. 4, pp. 403–409, Feb. 2011.

[36]. K. Prince, T. B. Gibbon, R. Rodes, E. Hviid, C. I. Mikkelsen, C. Neumeyr, M. Ortsiefer, E. Rönneberg, J. Rosskopf, P. Öhlén, E. In de Betou, B. Stoltz, E. Goobar, J. Olsson, R. Fletcher, C. Abbott, M. Rask, N. Plappert, G. Vollrath, and I. T. Monroy, "GigaWaM—Next-Generation WDM-PON enabling gigabit per-user data bandwidth," *IEEE J. Lightwave Technol.*, vol. 30, no. 10, pp. 1444-1454, May. 2012.

[37]. S.-M. Lee, K.-M. Choi, S.-G. Mun, J.-H. Moon, and C.-H. Lee, "Dense WDM-PON based on wavelength-locked Fabry-Pérot laser diodes," *IEEE Photon. Technol. Lett.*, vol. 17, no. 7, pp. 1067–1069, July 2005.

[38]. J. Shin, D. K Jung, J. K. Lee, J. H. Lee, Y. H. Choi, Y. C. Bang, H. S. Shin, J. Lee, S. T. Hwang, and Y. J. Oh, "155 Mbit/s transmission using ASE-injected Fabry-Pérot laser diode in WDM-PON over 70 ^{o}C temperature range," *IEE Electron. Lett.*, vol. 39, no. 18, pp. 1331–1332, Sep. 2003.

[39]. S.-G. Mun, J.-H. Moon, H.-K. Lee, J.-Y. Kim, and C.-H. Lee, "A WDM-PON with a 40 Gb/s (32 × 1.25 Gb/s) capacity based on wavelength-locked Fabry-Pérot laser diodes," *Opt. Express*, vol. 16, no. 15, pp. 11361–11368, July 2008.

[40]. J. H. Lee, C. H. Kim, Y. G. Han, and S. B. Lee, "WDM-based passive optical network upstream transmission at 1.25 Gb/s using Fabry–Perot laser diodes injected with spectrum-sliced, depolarized, continuous-wave supercontinuum source," *IEEE Photon. Technol. Lett*., vol. 18, no. 20, pp. 2108–2110, Oct. 2006.

[41]. K.-Y. Park and C.-H. Lee, "Intensity noise in a wavelength-locked Fabry–Perot laser diode to a spectrum sliced ASE," *IEEE J. Quantum Electron.*, vol. 44, no. 3, pp. 209–215, Mar. 2008.

[42]. Y. J. Wen and C. J. Chae, "WDM-PON upstream transmission using Fabry–Pérot laser diodes externally injected by polarization-insensitive spectrum-sliced supercontinuum pulses," *Opt. Comm.,* vol.260, no. 2, pp. 691-695, Apr. 2006.

[43]. Y.-S. Liao and G.-R. Lin, "22-channel detuning capacity of a side-mode injection locked FPLD for directly modulated 2.5 Gbit/s DWDM-PON," in *Proc. OFC/NFOEC*, paper OMS8, 2007.

[44]. Z. Xu, Y.- J. Wen, W.-D. Zhong, C.-J. Chae, X.-F. Cheng, Y. Wang, C. Lu, and J. Shankar, "High-speed WDM-PON using CW injection-locked Fabry-Pérot laser diodes," *Opt. Express*, vol. 15, no. 6, pp. 2953–2962, Mar. 2007.

[45]. Y. Katagiri, K. Suzuki, and K. Aida, "Intensity stabilization of spectrum-sliced Gaussian radiation based on amplitude squeezing using semiconductor optical

amplifiers with gain saturation," *IEE Electron. Lett.*, vol. 35, no. 16, pp. 1362–1364, Aug. 1999.

[46]. H. S. Shin, D. K. Jung, D. J. Shin, S. B. Park, J. S. Lee, I. K. Yun, S. W. Kim, Y. J. Oh, and C. S. Shim, "16 x 1.25 Gbit/s WDM-PON based on ASE-injected R-SOAs in 60 ºC temperature range," in *Proc. OFC/NFOEC*, paper OTuC5, 2006.

[47]. S.-B. Park, D. K. Jung, D. J. Shin, H. S. Shin, I. K. Yun, J. S. Lee, Y. K. Oh, and Y. J. Oh, "Colorless operation of WDM-PON employing uncooled spectrum-sliced reflective semiconductor optical amplifiers," *IEEE Photon. Technol. Lett*., vol. 19, no. 4, pp. 248–250, Feb. 2007.

[48]. K. Y. Cho, Y. Takushima, K. R. Oh, and Y. C. Chung, "Operating wavelength range of 1.25-Gb/s WDM PON implemented by using RSOA's," in *Proc. OFC/NFOEC*, paper OTuH3, 2008.

[49]. D. C. Kim, B.-S. Choi, H.-S. Kim, K. S. Kim, O-K. Kwon, and D.-K. Oh, "2.5 Gbps operation of RSOA for low cost WDM-PON sources," in *Proc. ECOC*, Sep. 20–24, paper P2.14, 2009.

[50]. A. Borghesani, I. F. Lealman, A. Poustie, D. W. Smith, and R. Wyatt, "High temperature, colourless operation of a reflective semiconductor optical amplifier for 2.5 Gbit/s upstream transmission in a WDM-PON," in *Proc. ECOC*, 2007.

[51]. P. Chanclou, F. Payoux, T. Soret, N. Genay, R. Brenot, F. Blache, M. Goix, J. Landreau, O. Legouezigou, and F. Mallécot, "Demonstration of RSOA-based remote modulation at 2.5 and 5 Gbit/s for WDM PON," in *Proc. OFC/NFOEC*, paper OWD1, 2007.

[52]. K. Y. Cho, S. P. Jung, A. Murakami, A. Agata, Y. Takushima, and Y. C. Chung "Recent progresses in RSOA-based WDM PON," in *Proc. ICTON,* paper Tu.D5.2, 2009.

[53]. K. Y. Cho, Y. Takushima, Y. C. Chung, "10-Gb/s operation of RSOA for WDM PON," *IEEE Photon. Technol. Lett.*, vol. 20, no. 18, pp. 1533-1535, 2008.

[54]. K. Y. Cho, A. Agata, Y. Takushima, and Y. C. Chung, "FEC optimization for 10-Gb/s WDM PON implemented by using bandwidth-limited RSOA", in *Proc. OFC/NFOEC*, paper OMN5, 2009.

[55]. H. Takesue and T. Sugie, "Wavelength channel data rewrite using saturated SOA modulator for WDM networks with centralized light sources," *IEEE J. Lightwave. Technol.*, vol. 21, no. 11, pp. 2546–2556, Nov. 2003.

[56]. Y. Y. Won, H. C. Kwon, and S. K. Han, "OBI noise reduction using gain saturated SOA in reflective SOA based WDM/SCM-PON optical links," *IEE Electron. Lett.*, vol. 42, no. 17, pp. 992-993, Aug. 2006.

[57]. T. Y. Kim, J. M. Kang, and S. K. Han, "Performance analysis of bidirectional hybrid WDM/SCM-PON link based on reflective semiconductor optical amplifier," *Microwave Opt. Technol. Lett.*, vol. 48, no. 11, pp. 2306–2309, Aug. 2006.

[58]. J. M. Kang and S. K. Han, "A novel hybrid WDM/SCM-PON sharing wavelength for up- and downlink using reflective semiconductor optical amplifier," *IEEE Photon. Technol. Lett.*, vol.18, no. 3, pp. 502–504, Feb. 2006.

[59]. L. Xu and H. K. Tsang, "WDM-PON using differential-phase-shift-keying remodulation of dark return-to-zero downstream channel for upstream," *IEEE Photon. Technol. Lett.*, vol.20, no. 10, pp. 833–835, May 2008.

[60]. B. Huang, X. Wang, Y. Liang, H. Liu, L. Wang, D. Huang, and N. Chi, "A novel re-modulation method in a WDM-PON with enhanced extinction ratio," in *Proc. ECOC*, Sep. 21–25, paper Th.1.F.3, 2008.

[61]. J. Xu and L.-K. Chen, "A new remodulation scheme for WDM-PONs with enhanced tolerance to chromatic dispersion and remodulation misalignment," *IEEE Photon. Technol. Lett.*, vol.22, no. 7, pp. 456–458, April 2010.

[62]. G.-W. Lu, N. Deng, C.-K. Chan, L.-K. Chen, "Use of downstream inverse-RZ signal for upstream data re-modulation in a WDM passive optical network," in *Proc. OFC/NFOEC*, paper OFI8, 2005.

[63]. B. K. Kim, H. Park, S. J. Park, and K. J. Kim, "Optical access network scheme with downstream Manchester coding and upstream NRZ remodulation," *IEE Electron. Lett.,* vol. 42, no. 8, pp. 484-485, April 2006.

[64]. Y. C. Chung, D. K. Jung, C. J. Youn, and H. G. Woo, "Spectrum-sliced bidirectional WDM PON," in *Proc. OFC/NFOEC*, paper WJ6- 1, 2000.

[65]. K. H. Han, E. S. Son, H. Y. Choi, K.W. Lim, and Y. C. Chung, "Bidirectional WDM PON using light-emitting diodes spectrum-sliced with cyclic arrayed-waveguide grating," *IEEE Photon. Technol. Lett.*, vol. 16, no. 10, pp. 2380–2382, Oct. 2004.

[66]. B. Schrenk, J. A. Lazaro, C. Kazmierski and J. Prat, "Colourless FSK/ASK Optical Network Unit based on a Fabry Pérot type SOA/REAM for symmetrical 10 Gb/s WDM-PONs," in *Proc. ECOC*, Sep. 20–24, paper 7.5.6, 2009.

[67]. D. Smith, I. Lealman, X. Chen, D. Moodie, P. Cannard, J. Dosanjh, L. Rivers, C. Ford, R. Cronin, T. Kerr, L. Johnston, R. Waller, R. Firth, A. Borghesani, R. Wyatt and A. Poustie, "Colourless 10Gb/s reflective SOA-EAM with low polarization sensitivity for long-reach DWDM-PON networks," in *Proc. ECOC*, Sep. 20–24, paper 8.6.3, 2009.

[68]. J. Bauwelinck, B. Schrenk, C. Kazmierski, J. A. Lazaro, J. Prat, and X. Z. Qiu, "Multi-operability and dynamic bandwidth allocation in PONs with electrically reconfigurable SOA/REAM-based ONUs," in *Proc. ECOC*, Sep. 19–23, paper Th.10.B.4, 2010.

[69]. S. Hann, T.-Y. Kim, and C.-S. Park, "Direct-modulated upstream signal transmission using a self-injection locked F-P LD for WDM-PON," in *Proc. ECOC*, paper We3.3.3, 2005.

[70]. E. Wong, K.-L. Lee and T. Anderson, "Low-cost WDM passive optical network with directly-modulated self-seeding reflective SOA," *IEE Electron. Lett.*, vol. 42, no. 5, pp. 1181–1182, March 2006.

[71]. M. Presi and E. Ciaramella, "Stable self-seeding of R-SOAs for WDM-PONs," in *Proc. OFC/NFOEC*, paper OMP4, 2011.

[72]. N. Cheng and F. Effenberger, "WDM-PON: Systems and Technologies," *ECOC workshop*, Turino, Italy, 2010.

[73]. G. P. Agrawal, "Fiber-optic communication systems," John Wiley & Sons, Inc., ISBN: 0-471-22114-7, (3rd Ed.) 2002.

[74]. J. D. Downie, A. B. Ruffin, and J. Hurley, "Ultra-low-loss optical fiber enabling purely passive 10 Gb/s PON systems with 100 km length," *Opt. Express*, vol. 17, no. 4, pp. 2392–2399, Feb. 2009.

[75]. Available: http://www.corning.com/opticalfiber/products/SMF-28_ULL_fiber.aspx

[76]. G. J. Pendock and D. D. Sampson, "Transmission performance of high bit rate spectrum-sliced WDM systems," *IEEE J. Lightwave. Technol.*, vol. 14, no. 10, pp. 2141–2148, Oct. 1996.

[77]. H. Kim, S. Kim, S. Hwang, and Y. Oh, "Impact of dispersion, PMD, and PDL on the performance of spectrum-sliced incoherent light sources using gain-saturated semiconductor optical amplifiers," *IEEE J. Lightwave. Technol.*, vol. 24, no. 2, pp. 775–785, Feb. 2006.

[78]. C. H. Kim, J. H. Lee, D. K. Jung, Y.-G. Han, and S. B. Lee, "Performance comparison of directly-modulated, wavelength-locked Fabry-Pérot laser diode and EAM-modulated spectrum-sliced ASE source for 1.25 Gb/s WDM-PON," in *Proc. OFC/NFOEC*, paper JWA82, 2007.

[79]. N. Cheng and F. Effenberger, "System impairments and performance implications of ASE seeded WDM PON systems," in *Proc. OFC/NFOEC*, paper NTuB2, 2011.

[80]. C. H. Kim, "Impact of seed source power on dispersion-limited maximum reach in WDM-PONs using broadband light source seeded optical sources," *Opt. Express*, vol. 20, no. 4, pp. 3473–3478, Feb. 2012.

[81]. J. H. Han, J. W. Ko, J. S. Lee, and S. Y. Shin, "0.1-nm narrow bandwidth transmission of a 2.5 Gb/s spectrum-sliced incoherent light channel using an all-optical bandwidth expansion technique at the receiver," *IEEE Photon. Technol. Lett.*, vol. 10, no. 10, pp. 1501–1503, Oct. 1998.

[82]. A. D. McCoy, P. Horak, B. C. Thomsen, M. Ibsen, and D. J. Richardson, "Noise suppression of incoherent light using a gain-saturated SOA: implications for spectrum-sliced WDM systems," *IEEE J. Lightwave. Technol.*, vol. 23, no. 8, pp. 2399–2409, Aug. 2005.

[83]. W. Lee, S.-H. Cho, J. Park, B. Kim, and B. Kim, "Noise suppression of spectrum-sliced WDM-PON light sources using FP-LD," *ETRI Journal*, vol. 27, no. 2, April 2005.

[84]. K.-M. Choi, J.-S. Baik, and C.-H. Lee, "Broadband light source using mutually injected Fabry–Pérot laser diodes for WDM-PON," *IEEE Photon. Technol. Lett.*, vol. 17, no. 12, pp. 2529–2531, Dec. 2005.

[85]. K.-M. Choi and C.-H. Lee, "A low-noise broadband light source for a WDM-PON based on mutually injected Fabry–Pérot laser diodes with RF modulation," *IEEE Photon. Technol. Lett.*, vol. 20, no. 24, pp. 2072–2074, Dec. 2008.

[86]. H. H. Lee, S.-H. Cho, and S. S. Lee, "Efficient excess intensity noise suppression of 100-GHz spectrum-sliced WDM-PON with a narrow-bandwidth seed light source," *IEEE Photon. Technol. Lett.*, vol. 22, no. 20, pp. 1542–1544, Oct. 2010.

[87]. R. Ramaswami and K. N. Sivarajan, "Optical Networks", second edition.

[88]. A. H. Hartog and M. P. Gold, "On the theory of backscattering in single-mode optical fibers", *IEEE J. Lightwave. Technol.*, vol. LT-2, no. 2, pp. 76-82, Apr, 1984.

[89]. G. Talli, C. W. Chow and P. D. Townsend, "Filter impact in spectrally-broadened Rayleigh noise reduction schemes for DWDM-PONs," in *Proc. OFC/NFOEC*, paper OWD4, 2007.

[90]. J. A. Lazaro, C. Arellano, V. Polo, and J. Prat, "Rayleigh scattering reduction by means of optical frequency dithering in passive optical networks with remotely seeded ONUs," *IEEE Photon. Technol. Lett.*, vol. 19, no. 2, pp. 64–66, Jan. 2007.

[91]. A. Murakami1, H. C. Jeon, K. Y. Cho, A. Agata, Y. Takushima, Y. C. Chung, and Y. Horiuchi, "Reflection tolerance enhancement of RSOA-based WDM PON by using optical frequency dithering," in *Proc. OFC/NFOEC*, paper OMN4, 2009.

[92]. E. K. MacHale, G. Talli, C. W. Chow and P. D. Townsend, "Reduction of signal-induced Rayleigh noise in a 10Gb/s WDM-PON using a gain-saturated SOA," in *Proc. ECOC*, paper paper We7.6.3, 2007.

[93]. L. Banchi, R. Corsini, M. Presi, F. Cavaliere, and E. Ciaramella, "Enhanced reflection tolerance in WDM-PON by chirped RZ modulation," *IEE Electron. Lett.*, vol. 46, no. 14, pp. 1009–1011, July 2010.

[94]. A. Chiuchiarelli, M. Presi, R. Proietti, G. Contestabile, P. Choudhury, L. Giorgi, and E. Ciaramella, "Enhancing resilience to Rayleigh crosstalk by means of line coding and electrical filtering," *IEEE Photon. Technol. Lett.*, vol. 22, no. 1, pp. 85–87, Jan. 2010.

[95]. B. Schrenk, G. de Valicourt, J. A. Lazaro, R. Brenot, and J. Prat, "Rayleigh scattering tolerant PON assisted by four-wave mixing in SOA-based ONUs," *IEEE J. Lightwave Technol.*, vol. 28, no. 23, pp. 3364–3371, Dec. 2010.

[96]. S.-H. Cho, H. H. Lee, J. H. Lee, and S. S. Lee, "Reduction of back-reflection induced power penalty by means of coherent seeding source with optical feedback in a loop-back WDM-PON," in *Proc. OFC/NFOEC*, paper OMP3, 2011.

[97]. T. H. Wood, R. A. Linke, B. L. Kasper, and E. C. Carr, "Observation of coherent Rayleigh noise in single-source bidirectional optical fiber systems," *IEEE J. Lightwave Technol.*, vol. 6, no. 2, pp. 346–352, Feb. 1988.

[98]. P. Gysel and R. K. Staubli, "Spectral properties of Rayleigh backscattered light from single-mode fibers caused by a modulated probe signal," *IEEE J. Lightwave Technol.*, vol. 8, no. 12, pp. 1792–1798, Dec. 1990.

[99]. R. K. Staubli and P. Gysel, "Crosstalk penalities due to coherent Rayleigh noise in bidirectional optical communication systems," *IEEE J. Lightwave Technol.*, vol. 9, no. 3, pp. 375–380, March 1991.

[100]. M. Oskar van Deventer, "Power penalties due to reflection and Rayleigh backscattering in a single frequency bidirectional coherent transmission system," *IEEE Photon. Technol. Lett.*, vol. 5, no. 7, pp. 851–854, July 1993.

[101]. M. Feuer, M. Thomas, and L. Lunardi, "Backreflection and loss in single-fiber loopback networks," *IEEE Photon. Technol. Lett.*, vol. 12, no. 8, pp. 1106–1108, Aug. 2000.

[102]. J. Ko, S. Kim, J. Lee, S. Won, Y. S. Kim, and J. Jeong, "Estimation of performance degradation of bidirectional WDM transmission systems due to Rayleigh backscattering and ASE noises using numerical and analytical models," *IEEE J. Lightwave Technol.*, vol. 21, no. 4, pp. 938–946, Apr. 2003.

[103]. G. Talli, D. Cotter, and P. D. Townsend, "Rayleigh backscattering impairments in access networks with centralized light source," *IEE Electron. Lett.*, vol. 42, no. 15, pp. 877–878, July 2006.

[104]. C. H. Kim, K. Lee, and S. B. Lee, "Effects of in-band crosstalk in wavelength-locked Fabry–Perot laser-diode-based WDM PONs," *IEEE Photon. Technol. Lett.*, vol. 21, no. 9, pp. 596–598, May 2009.

[105]. M. Fujiwara, J. I. Kani, H. Suzuki, and K. Iwatsuki, "Impact of backreflection on upstream transmission in WDM single-fiber loopback access networks," *IEEE J. Lightwave Technol.*, vol. 24, no. 2, pp. 740–746, Feb. 2006.

[106]. E. T. Lopez, J. A. Lazaro, C. Arellano, V. Polo, and J. Prat, "Optimization of Rayleigh-limited WDM-PONs with reflective ONU by MUX positioning and optimal ONU gain," *IEEE Photon. Technol. Lett.*, vol. 22, no. 2, pp. 97–99, Jan. 2010.

[107]. U. H. Hong, K. Y. Cho, Y. Takushima, and Y. C. Chung, "Effects of Rayleigh backscattering in long-reach RSOA-based WDM PON," in *Proc. OFC/NFOEC*, paper OThG1, 2010.

[108]. C. Arellano, K.-D. Langer, and J. Prat, "Reflections and multiple Rayleigh backscattering in WDM single-fiber loopback access networks," *IEEE J. Lightwave Technol.*, vol. 27, no. 1, pp. 12–18, Jan. 2009.

[109]. Y. J. Lee, K. Y. Cho, A. Murakami, A. Agata, Y. Takushima, and Y. C. Chung, "Reflection tolerance of RSOA-based WDM-PON," in *Proc. OFC/NFOEC*, paper OTuH5, 2008.

[110]. K. Y. Cho, Y. J. Lee, H. Y. Choi, A. Murakami, A. Agata, Y. Takushima, and Y. C. Chung, "Effects of reflection in RSOA-based WDM PON utilizing remodulation Technique," *IEEE J. Lightwave Technol.*, vol. 27, no. 10, pp. 1286–1295, May 2009.

[111]. P. Wan and J. Conradi, "Impact of double Rayleigh backscatter noise on digital and analog fiber systems," *IEEE J. Lightwave Technol.*, vol. 14, no. 3, pp. 288–297, Mar. 1996.

[112]. B. W. Kang and C. H. Kim, "Limitation on gain of bidirectional amplifier in amplified WDM-PON using broadband light source seeded optical sources," in *Proc. Photonics Global Conference (PGC),* 2010.

[113]. N. Buldawoo, S. Mottet, H. Dupont, D. Sigogne, and D. Meichenin, "Transmission experiment using a laser amplifier-reflector for DWDM access network," in *Proc. ECOC*, Madrid, Spain, 1998, vol. 1, pp. 273–274.

[114]. R. W. Tkach and A. R. Chraplyvy, "Phase noise and linewidth in an InGaAsP DFB laser," *IEEE J. Lightwave. Technol.*, vol. LT-4, no. 11, pp. 1711–1716, Nov. 1986.

[115]. H. Hu and H. Anis, "Degradation of bi-directional single fiber transmission in WDM-PON due to beat noise," *IEEE J. Lightwave Technol.*, vol. 26, no. 8, pp. 870–881, Apr. 2008.

[116]. Available: http://www.lightwavestore.com/product_datasheet/OMS-LDS-Tune-L-020C_pdf1.pdf

[117]. Available: http://www.jdsu.com/en-us/Optical-Communications/Products/a-z-product- list/Pages/filter-tunable-voltage-controlled-100-and-50-ghz.aspx

[118]. Available: http://www.jdsu.com/en-us/Optical-Communications/Products/a-z-product- list/Pages/modulator-2-5-gbps-bias-ready-butterfly.aspx

[119]. Available: http://www.kamelian.com/products.html

[120]. Available: http://www.optoway.com.tw/index.html

[121]. R. Lang, "Injection locking properties of a semiconductor laser," *IEEE J. Quantum Electron.*, vol. 18, no. 6, pp. 976–983, June 1982.

[122]. X. J. Meng, T. Chau, and M. C. Wu, "Improved intrinsic dynamic distortions in directly modulated semiconductor lasers by optical injection locking," *IEEE Trans. Microwave Theory Tech.*, vol. 47, no. 7, pp. 1172–1176, July 1999.

[123]. S. Y. Kim, S. B. Jun, Y. Takushima, E. S. Son, and Y. C. Chung, "Enhanced performance of RSOA-based WDM PON by using Manchester coding," *J. Opt. Netw.*, vol. 6, no. 6, pp. 624–630, June 2007.